ELSEVIER

Tectonophysics 284 (1998) 31–63

TECTONOPHYSICS

Deep-imaging seismic and gravity results from the offshore Cameroon Volcanic Line, and speculation of African hotlines [1]

Jayson B. Meyers [a,*], Bruce R. Rosendahl [a], Christopher G.A. Harrison [a], Zan-Dong Ding [a]

[a] *Marine Geology and Geophysics, University of Miami–RSMAS, Miami, FL 33149, USA* [2]

Received 27 January 1997; revised version received 5 June 1997; accepted 5 June 1997

Abstract

Deep-imaging multi-channel seismic reflection data show that volcanic centers along the offshore part of the Cameroon Volcanic Line (CVL) are composed of uplifted, Aptian to Late Cretaceous oceanic crust, >4 km of sedimentary overburden, and Neogene igneous rocks, with volcanic material forming a cap <1.5 km thick over pre-uplift sedimentary deposits. At Príncipe Island, the underlying oceanic basement has been uplifted by as much as 3 km to form a crustal arch less than 200 km wide perpendicular to the CVL trend. Vertical faults having small offsets and dikes are common across this arch. Reflection Moho shallows parallel to the uplifted crust along margins of the arch, but is not observed directly below the arch axis where volcanism and faulting are pervasive. The episode of crustal uplift is marked by a prominent reflection unconformity. This unconformity occurs at other CVL islands and seamounts and represents a synchronous period of crustal uplift and volcanism. Reflectors from this unconformity have been correlated to offshore boreholes indicating a Miocene age. Gravity modelling indicates that an elongate wedge of relatively less dense lithospheric mantle ($\Delta\rho = -0.1$ g/cm^3) underlies Príncipe Island to a depth of 40 km. This interpreted zone of lighter mantle material may form by a combination of intruded mafic partial melt and reheating of the lithosphere. Dynamic support from asthenospheric upwelling may also have contributed to uplift. Other NE-trending volcanic chains and rises off West Africa (Canary Islands, Cape Verde Rise, Sierra Leone Rise and Walvis Ridge) display similar features to CVL islands. These volcanic chains exhibit crustal uplift unconformities and intraplate volcanism occurring during the Miocene and later; Miocene and older marine sediments crop out on most of the islands; there are no flexural depressions surrounding volcanic centers; their ocean island basalts (OIB) have similar geochemical characteristics; the OIB does not appear to be the main construction material of each chain; anomalously high modern heatflow occurs along their lengths; and hotspot-like age progression of volcanism is not clearly defined along their lengths.It is apparent that the CVL is not the product of a single mantle plume or hotspot, and we speculate that the CVL and possibly other NE-trending volcanic chains off West Africa (and perhaps linear belts of Neogene volcanism on the African continent) are the result of linear, mantle upwelling zones or 'hotlines'. These hotlines are suggested to form above upwelling flow currents in between cylindrical Rayleigh–Bernard convection rolls in the upper mantle. Such convection may be driven by heat transfer across and/or shear along the 670 km discontinuity as a result of convection in the lower mantle.

Keywords: Cameroon; seismic; geophysics; South Atlantic; West Africa; volcanic island; mantle convection

* Corresponding author. Present address: Astro Mining, 46 Kings Park Rd., West Perth, W.A. 6005, Australia. Tel.: +61-9-3278278; fax: +61-9-3222033.

[1] J.B. Meyers, B.R. Rosendahl and Zan-Dong Ding: collaborators in Project PROBE (Proto-Rifts and Ocean Basin Evolution).

[2] Tel.: +1-305-3614610; fax: +1-305-3614636.

0040-1951/98/$19.00
PII S0040-1951(97)00173-X

1. Introduction

The Cameroon Volcanic Line (CVL) is a linear trend of intraplate, mafic alkali volcanic centers and fissures striking 030°, crossing from Proterozoic Pan African basement in central Cameroon and southern Nigeria to oceanic crust as far as Pagalu Island in the equatorial Atlantic; and perhaps extending more westerly to St. Helena Island (Fig. 1). Mount Cameroon is the best known volcano along the CVL and it has been active during this century. The first comprehensive geological study of the CVL was carried out by Hedberg (1969).

Alignment of volcanic centers along the CVL has led to the concept that it forms a hotspot trace recording rotation of the African plate over a relatively fixed mantle source presently underlying St. Helena Island (Morgan, 1972, 1983; Duncan and Richards, 1991; O'Connor and Le Roex, 1992). Most isotopic ages from volcanic rocks erupted along the CVL fall within the Miocene, although older (30 Ma, Late Oligocene) and younger dates have been reported (Hedberg, 1969; Grunau et al., 1975; Piper and Richardson, 1972; Dunlop and Fitton, 1979; Cornen and Maury, 1980; Fitton and Dunlop, 1985; Halliday et al., 1988). Sills, lava flows and volcaniclastics are found interbedded with Miocene age shelf sediments offshore of Cameroon, near Bioko (Regnoult, 1986). The ages of CVL rocks do not, however, show progressive SW-directed younging expected for migration of the African plate over a stationary mantle plume (Burke and Wilson, 1972). In fact, there is no evidence of migration of volcanic centers along the CVL, nor any evidence in multi-channel (MCS) data shown here for volcanism occurring between the time Aptian oceanic basement was formed to onset of CVL volcanism in the Oligocene (see also Meyers and Rosendahl, 1991).

In this paper deep-imaging MCS and potential field data from the West African PROBE Study (WAPS) are used to examine Príncipe Island, along the CVL (Fig. 1). WAPS MCS data clearly demonstrate that the offshore CVL is comprised of uplifted, Aptian to Late Cretaceous oceanic basement, thick pre-CVL volcanism sedimentary overburden, Oligocene and younger volcanic rocks intermixed with sediments, and onlapping deep-water sediments. These volcanic rocks account for only a small percentage of the total mass comprising the islands of Príncipe, São Tomé and Bioko, and the seamount between Bioko and Príncipe (Meyers and Rosendahl, 1991).

Modelling of the gravity field in this paper suggests that a mass deficit underlies the island. This mass deficit is not related to flexural downwarp surrounding the islands, and is suggested to represent a linear wedge of hot, mafic intruded lithospheric mantle.

We do not consider the CVL to represent a typical hotspot trace, and in this paper we then compare our observations to published results from other West African island chains (Canary Islands, Cape Verde Islands, Sierra Leone Rise, Walvis Ridge) that share many geological and geochemical characteristics. The striking similarities between all of these West African island chains cause us to speculate that they have formed above mantle hotlines, an idea proposed by (Bonatti and Harrison, 1976; Bonatti et al., 1977) for similar volcanic lines in the Pacific.

In light of MCS data shown here, the hypothesis of Herman et al. (1977), which originally suggested that South Atlantic hotlines represent upwelling zones formed in between upper mantle convection rolls, can adequately explain the origin of the CVL and geochemistry of its ocean island basalt (OIB). We build upon this hypothesis, invoking shear along and/or heat transfer across the 670 km discontinuity as a driving mechanism for these convective rolls.

2. Background

CVL volcanic rocks are almost identical geochemically in both oceanic and continental regions. They are dominantly alkali-rich OIB, having identical trace element abundances, enriched large-ion lithophile elements (LILE) and radiogenic Sr and Pb in relation to mid-ocean ridge basalt (MORB), implying a related, upper mantle source from somewhere above the 670 km discontinuity (Fitton, 1983; Fitton and Dunlop, 1985; Halliday et al., 1988). High $^{206}Pb/^{204}Pb$ ratios (>19) are documented from CVL lavas over a broad area centered at the presumed transition between oceanic and continental crust (Halliday et al., 1990), but relatively high $^{206}Pb/^{204}Pb$ ratios continue out to St. Helena Island, signifying a similar mantle source (White, 1985).

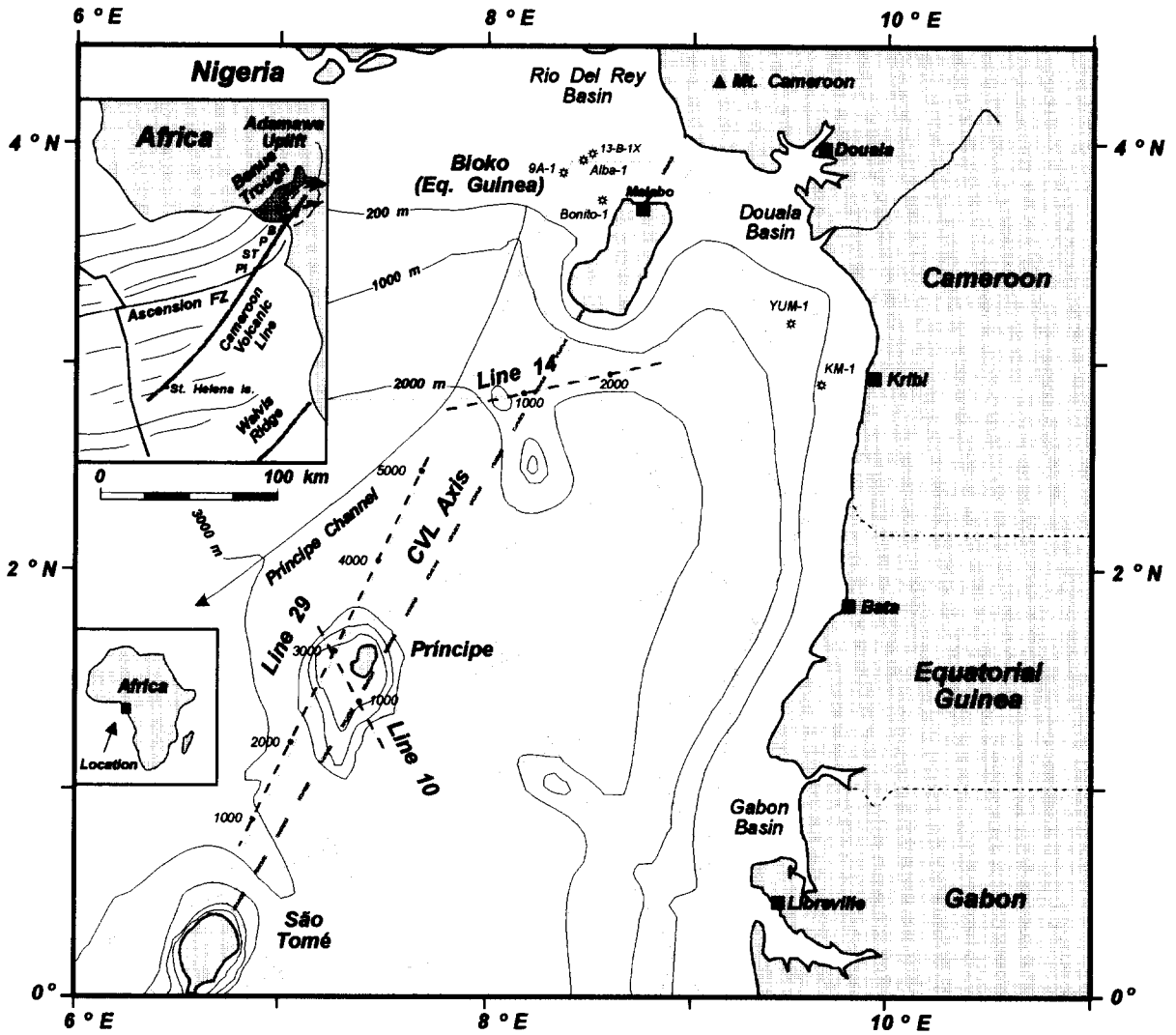

Fig. 1. Location map of West African PROBE Study (WAPS) MCS coverage (dotted lines) and Cameroon Volcanic Line (CVL) islands. Dashed portions of MCS track-lines with field file numbers are shown in Figs. 2–4 and 6. Offshore wells that tie to WAPS MCS profiles are also shown. *Line 29* runs sub-parallel to the *CVL Axis*, whereas *Line 10* crosses it. Plot is universal transverse mercator projection centered at 9°E.

The high $^{206}Pb/^{204}Pb$ ratios observed in CVL basalts sampled near the oceanic–continental crustal transition are believed to have been produced by reheating or entrainment of upper mantle material that is approximately 125 Ma old (Halliday et al., 1990), roughly coincident with initial rifting in this part of the Atlantic (Meyers et al., 1996).

Fitton (1980) proposed that the CVL represents a Y-shaped zone of asthenospheric upwelling that produced rifting of the Benue Trough–Yola Rift system during Albian to Late Cretaceous times (Fig. 1). He theorized that this Y-shaped zone of upwelling was reestablished under the present location of the CVL after 7° of clockwise rotation of the African Plate with respect to this upwelling zone about a pole in Sudan; although admitting that there was no evidence for counterclockwise migration of volcanism north of the CVL and that polar wander curves for the African Plate lacked the resolution needed to test this idea. He instead based his hypothesis on the sim-

ilarity in shape of the Cretaceous Benue Trough and Tertiary CVL and geochemical similarity to some rift-related volcanic rocks.

Within the onshore portion of the CVL, pre-volcanic crust is uplifted >1 km into a NE-trending dome called the Adamawa uplift (Fig. 1), which is suspected to be underlain by a mantle thermal anomaly (Reyre, 1966; Fitton, 1983; Stuart et al., 1985; Fairhead, 1988; Okereke, 1988). Mount Cameroon overlies the southwestern flank of this crustal uplift zone, and is bounded to the north and south by the Rio Del Rey and Douala basins, respectively (Fig. 1). Cretaceous sedimentary units in the onshore parts of these basins trend northwest on either side of Mt. Cameroon, and Mt. Cameroon volcanics are believed to intrude and overlie ~800 m of sedimentary deposits that once were shared by these basins (Dumort, 1968; Hedberg, 1969; Regnoult, 1986). On the flanks of Mt. Cameroon, marine shales of Miocene age crop out below lava flows at an elevation of 300 m above sea level (Hedberg, 1969; Regnoult, 1986; Déruelle et al., 1987).

Meyers and Rosendahl (1991) proposed that the Adamawa uplift and the islands of São Tomé, Príncipe and Bioko were formed during a synchronous phase of crustal uplift and volcanism in the Miocene. They recognized a Miocene uplift unconformity along the flanks of volcanic centers, and suggested that volcanism began in the Oligocene, with the main phase of volcanism and crustal uplift ensuing in the Miocene, although minor volcanism has continued into the Holocene. They also showed that the crust under volcanic centers in the offshore portion of the CVL has been uplifted by >3 km, in places, to form NE-trending asymmetric arches with steep, SE-dipping limbs. Submarine volcanism onto and igneous intrusion into deep sea sediments, and subtle asymmetric arching of the crust also have been observed in saddles between volcanic centers (Hedberg, 1969; Grunau et al., 1975; Regnoult, 1986; Meyers and Rosendahl, 1991). Miocene age for crustal uplift is coincident to Miocene ages for well established volcanic centers on both the continental and oceanic portions of the CVL (Grunau et al., 1975; Fitton and Dunlop, 1985; Regnoult, 1986; Déruelle et al., 1987; Halliday et al., 1988). Uplift of crust also helps explain the existence of small windows of Miocene and older, deep-water marine sediments below volcanic flows on several CVL islands, and below the flanks of Mt. Cameroon.

Coeval volcanism and crustal uplift along the CVL implies that the CVL is a manifestation of discrete volcanic centers formed along a mantle hotline (cf. Bonatti and Harrison, 1976). This idea that the CVL and other South Atlantic chains formed over hotlines was first proposed by Herman et al. (1977), based upon the anomalously high heatflow associated with these linear trends of volcanism.

While the CVL appears to be a linear trend of volcanism and uplift, and not a hotspot trace, the explanation for the spacing and timing of the main eruptive centers along the CVL is not clear. The linear trend of volcanic centers strikes slightly more northerly than NE-trending fracture zones off West Africa (Fig. 5; Burke, 1969; Emery et al., 1975; Sibuet and Mascle, 1978; Meyers et al., 1996), which has led some workers to consider that the spacing of CVL seamounts and islands is related to fracture zone crossings (Vogt, 1974; Meyers and Rosendahl, 1991). Remnants of the Central African shear zone and a pre-break-up shear zone cross through the Adamawa uplift and have the same trend as offshore islands. The similarity in shear orientation has led other workers to hypothesize that the CVL is a manifestation of a reactivated, sinistral lithospheric shear system (Reyre, 1966; Moreau et al., 1987; Déruelle et al., 1987; Fairhead, 1988).

3. Methods

WAPS MCS data were acquired in 1989 aboard the M/V *GECO-PRAKLA Tau*. Navigation was by GPS and doppler sonar dead reckoning. Gravity and magnetic data also were collected during MCS data acquisition by ARK Geophysical. The gravity data were digitally recorded using a LaCoste-Romberg 592 air/sea gravimeter, base-tied to Port Gentil, Gabon, and corrected for latitude and Eotvos effect and filtered with a 2.5 km low pass cosine tapered boxcar filter. Marine magnetometer data were digitally recorded, edited for noisy spikes, filtered using a 1.5 km low pass cosine tapered boxcar filter, and the 1989 International Geomagnetic Reference Field was subtracted.

WAPS MCS data acquisition parameters permitted seismic penetration below reflective volcanic ma-

terial and useful stacking velocity information below the sedimentary column to reflection Moho. The source was an array of 36 air-guns, in six sub-arrays, totalling 7524 in^3 in volume, towed at 8.5 m depth. The active streamer length was 6000 m (group interval 50 m, 120 channels, 20 m depth). The near offset was 1000 m from the center of the source, the far offset was 7000 m. Shot interval was 50 m, with a 25 m common mid-point (CMP) interval. Data were recorded in SEG D, at 4 ms sample rate, to 20 s two-way travel time (TWTT), and filtered; the low cut-off was 3.5 Hz, the high cut-off was 90 Hz. Data were demultiplexed, resampled to 8 ms and 16 s record lengths, corrected for spherical divergence, trace equalized over 7–15 s, dip-moveout (DMO) corrected from normal-moveout (NMO) velocity spectra every 10 km, and predictively deconvolved (window length of 296 ms and gap of 64 ms). Semblance velocity analyses were picked about every 3 km, NMO corrected from the same velocity spectra, muted by NMO stretch, CMP stacked to 60 fold, trace normalized for far offset, post-stack predictively deconvolved (2 windows of 296 ms and gaps of 64 and 200 ms), trace mixed, band-pass filtered, and phase-shift migrated using a single velocity function for each line segment (~125 km long). Line segments were merged after migration, automatic gain control (AGC) was applied with a window length of 2 s, and the data were F-K dip filtered.

4. Data and results

4.1. Oceanic basement

Crystalline basement around and under São Tomé and Príncipe has reflection geometry typical of oceanic crust. Hyperbolic reflections in unmigrated MCS profiles, interpreted as oceanic basement layer 2, occurs in crust surrounding CVL islands (Fig. 2; Grunau et al., 1975; Meyers and Rosendahl, 1991). Reflectors from layer 2 are shown in migrated profiles here to exhibit a relatively flat reflection surface that is commonly truncated by closely spaced faults

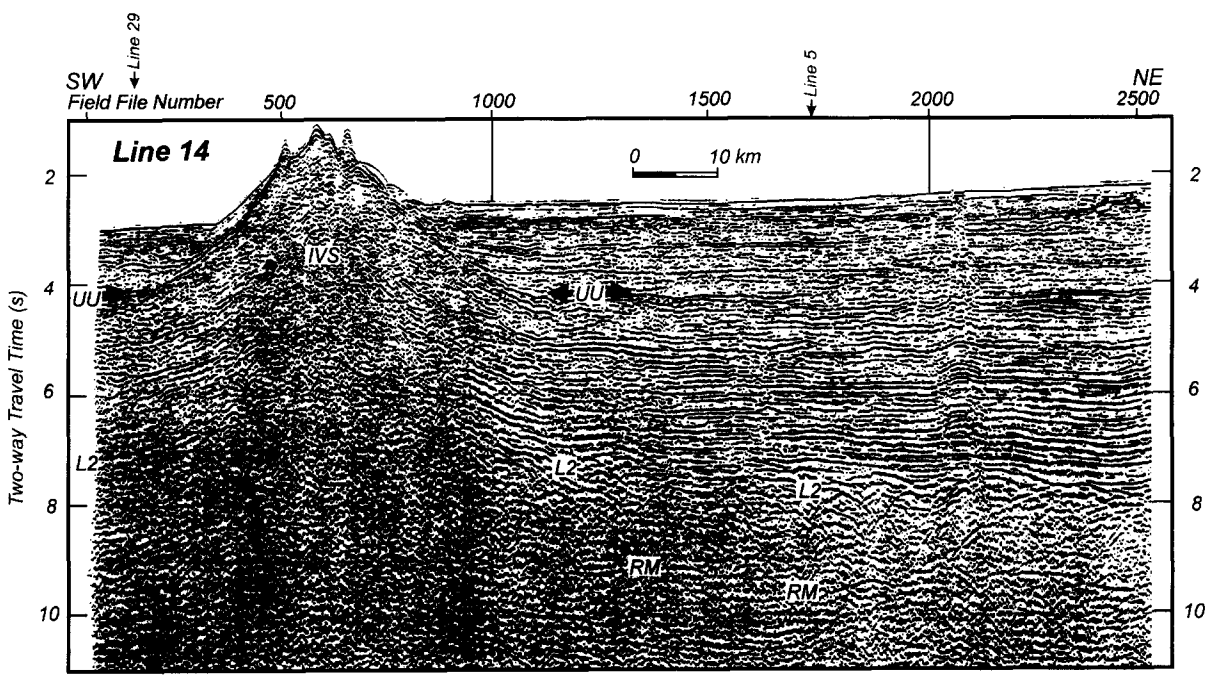

Fig. 2. Segment of unmigrated WAPS deep-imaging MCS Line 14 crossing the seamount between Bioko and Príncipe islands. Note how sedimentary reflections continue through the seamount indicating crustal uplift. *RM* = reflection Moho; *L2* = top of oceanic basement layer 2; *IVS* = intercalated volcanics and sediments; *UU* = uplift unconformity. See Fig. 1 for location and Section 3 for acquisition and processing parameters.

(Fig. 3). Reflection Moho is observed on these profiles 1.7–2.5 s TWTT below the top of interpreted layer 2 (Figs. 2–4). Where oceanic crust has not been disrupted by Neogene uplift and volcanism, the position of the reflection Moho is well constrained by a rapid increase in stacking velocities from 6.8–7.2 km/s at the base of interpreted oceanic crust, to 8.0–8.3 km/s below the reflection Moho boundary. Reflection Moho rises parallel or sub-parallel to the top of oceanic basement layer 2 and pre-uplift sediments beneath the flanks of this crustal arch (Figs. 3 and 4) and other CVL crustal uplifts (Meyers and Rosendahl, 1991). However, the location of reflection Moho directly under the axis Príncipe is impossible to identify (Figs. 3 and 4).

Figs. 3 and 4 also show that oceanic crust under the margins of Príncipe Island has been uplifted by >3 km, and possibly more immediately below the island; Fig. 2 shows ~3.5 km of uplift from the uplift unconformity 'UU' to the top of the seamount. This uplifted oceanic crust forms an arch, or elongated dome, less than 100 km wide along NW-oriented profiles and over 200 km long along NE–SW-oriented profiles running to the northwest of the CVL axis (Figs. 1, 3 and 4; Meyers and Rosendahl, 1991). Saddles between islands are also disrupted by faulting and reflectors interpreted to be Neogene volcanics (Meyers and Rosendahl, 1991).

4.2. Fracture zones

Away from the Príncipe crustal arch, normal faults offset the interpreted top of oceanic basement layer 2 and sedimentary reflectors, but this fault displacement dies out at 0.5 s TWTT above the top of oceanic basement (Fig. 3, field files 800–1200 and 3800–5000). The oceanic basement and reflection Moho between field files 3800 and 5000 on Line 29 (Fig. 3) have a large degree of seismic relief and range in thickness from 1.5–2.5 s TWTT. Structures within this zone appear to consist of two prominent highs bounded by asymmetric troughs filled with sediments. Normal faults within these troughs appear to have been active during SW-oriented progradation of sedimentary deposits that directly overlie basement, as indicated by downlap surfaces and rotation of faulted reflectors. Reflectors higher up in the section show no offset and lap onto structural highs, with the exception of the area over what appears to be a diapiric structure or fault zone at field file 4400 (Fig. 3). The observation that these faults die out in sedimentary reflectors 1 s TWTT above interpreted Layer-2 indicates that thermal readjustments and faulting of the oceanic basement continued for some time after creation of oceanic basement.

A set of normal faults with SW apparent dips is located between field files 800 and 1200 on Line 29 (Fig. 3). Here too, offset sedimentary reflectors are only observed immediately above oceanic basement. Small offsets of reflection Moho also occur, but the seismic topography of reflection Moho is not as variable as across the faulted crust between field files 3800–5000 (Fig. 3), and its crustal thickness is relatively uniform (~1.7 s TWTT). This area may represent a small fracture zone.

We interpret the region of faulted oceanic crust between field files 3800–5000 (Fig. 3) to represent a larger fracture zone that has been infilled by sediments and the oceanic lithosphere on both sides was thermally equilibrated though time. Formation of oceanic crust during the Cretaceous Quiet Period, burial beneath 3–5 s TWTT (>5 km) of sediments, and strong magnetic overprinting by Cameroon Line volcanics has produced weak magnetic basement signature at sea level. This helps to explain why the location of fracture zone trends east of 7°E longitude have not been mapped consistently (cf. Emery et al., 1975; Sibuet and Mascle, 1978). Mapping of the high relief oceanic crust and correlation to faults observed using gravity anomalies calculated from stacked Geosat and Seasat data (Fairhead and Binks, 1991; Binks and Fairhead, 1992) indicates that this zone is the buried, eastern extension of an unnamed fracture zone which we refer to here as the Cameroon Fracture Zone (Fig. 5). Similar, asymmetric basin geometries have been described across other South Atlantic fracture zones (Gorini and Bryan, 1976; Sibuet and Mascle, 1978), and possible zones of intraplate extension related to Santonian plate reorganizations off of West Africa (cf. Basile and Mascle, 1990). The Cameroon Fracture Zone was probably a prominent feature during Early Cretaceous rifting in the Douala basin, and this fracture zone likely formed the northernmost barrier to salt deposition in the Aptian proto-oceanic sea (Gorini and Bryan, 1976; Meyers et al., 1996).

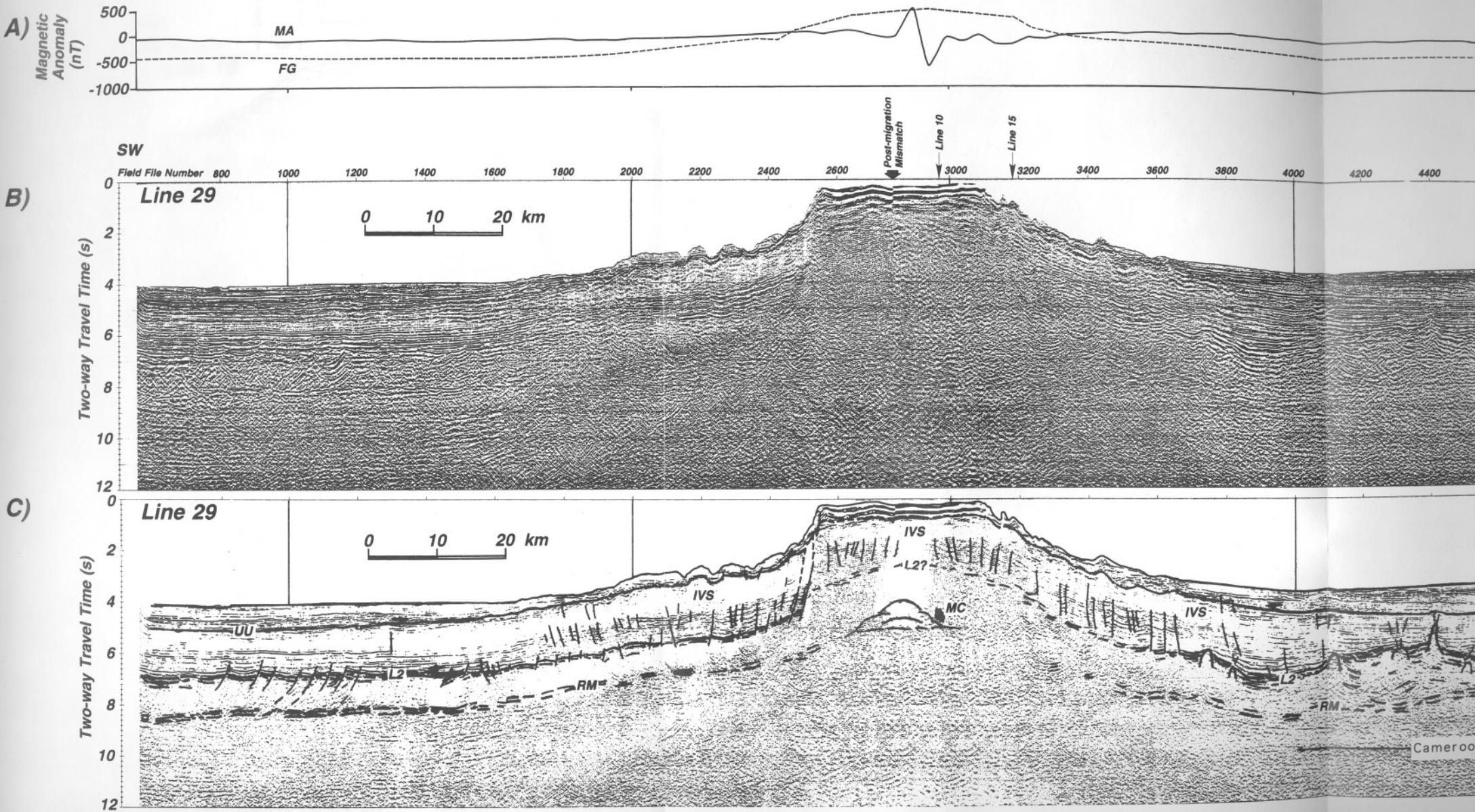
A)
Magnetic Anomaly (nT)
500
0
-500
-1000
MA
FG
B)
SW
Field File Number 800
1000
1200
1400
1600
1800
2000
2200
2400
2600
Post-migration Mismatch
Line 10
3000
Line 15
3200
3400
3600
3800
4000
4200
4400
Line 29
0 10 20 km
Two-way Travel Time (s)
0
2
4
6
8
10
12
C)
Line 29
0 10 20 km
IVS
L2?
MC
UU
L2
RM
Cameroo

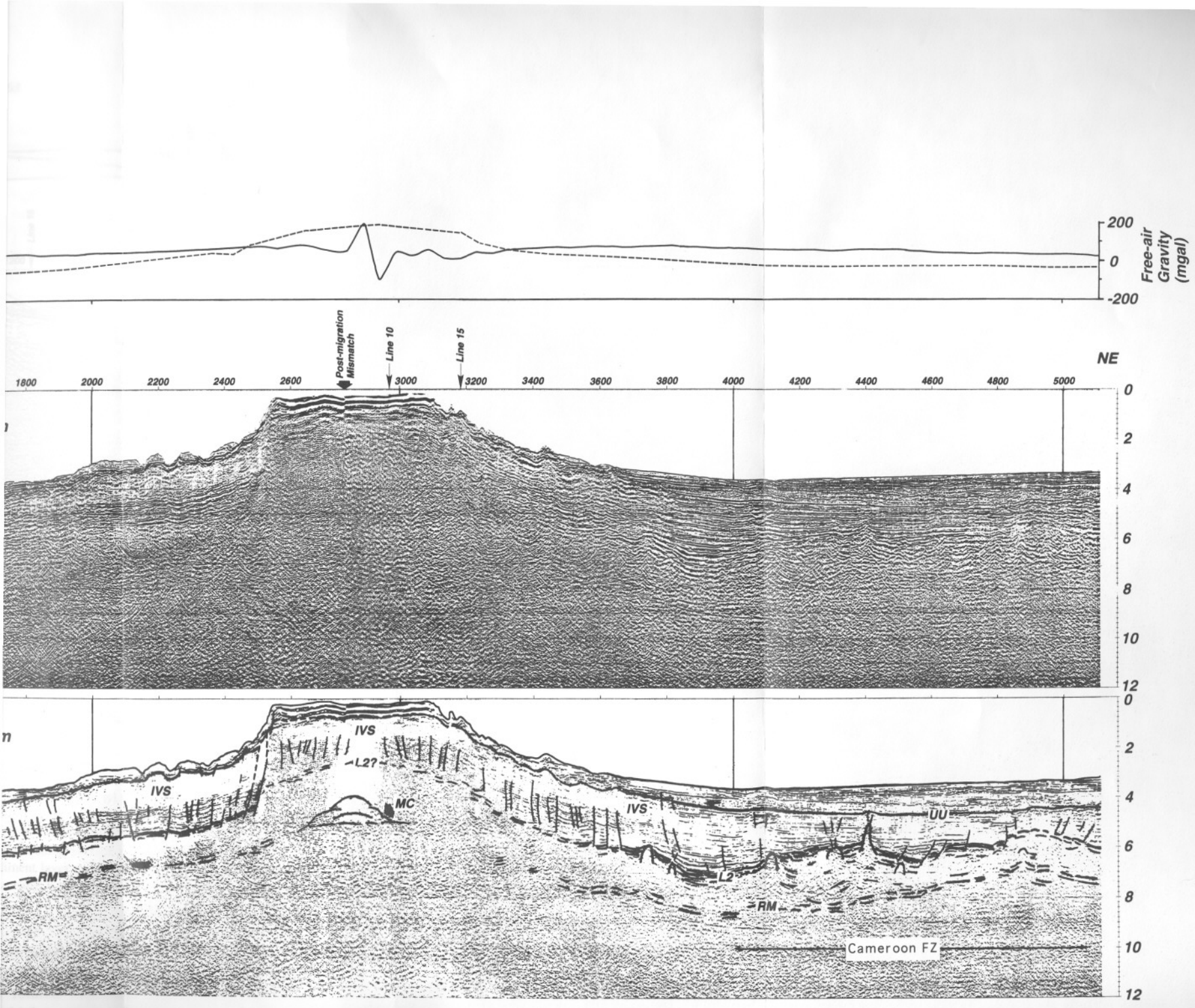
200
0
-200
Free-air Gravity (mgal)
Post-migration Mismatch
Line 10
Line 15
NE
1800
2000
2200
2400
2600
3000
3200
3400
3600
3800
4000
4200
4400
4600
4800
5000
0
2
4
6
8
10
12
IVS
L2?
MC
IVS
IVS
UU
L2
RM
RM
Cameroon FZ

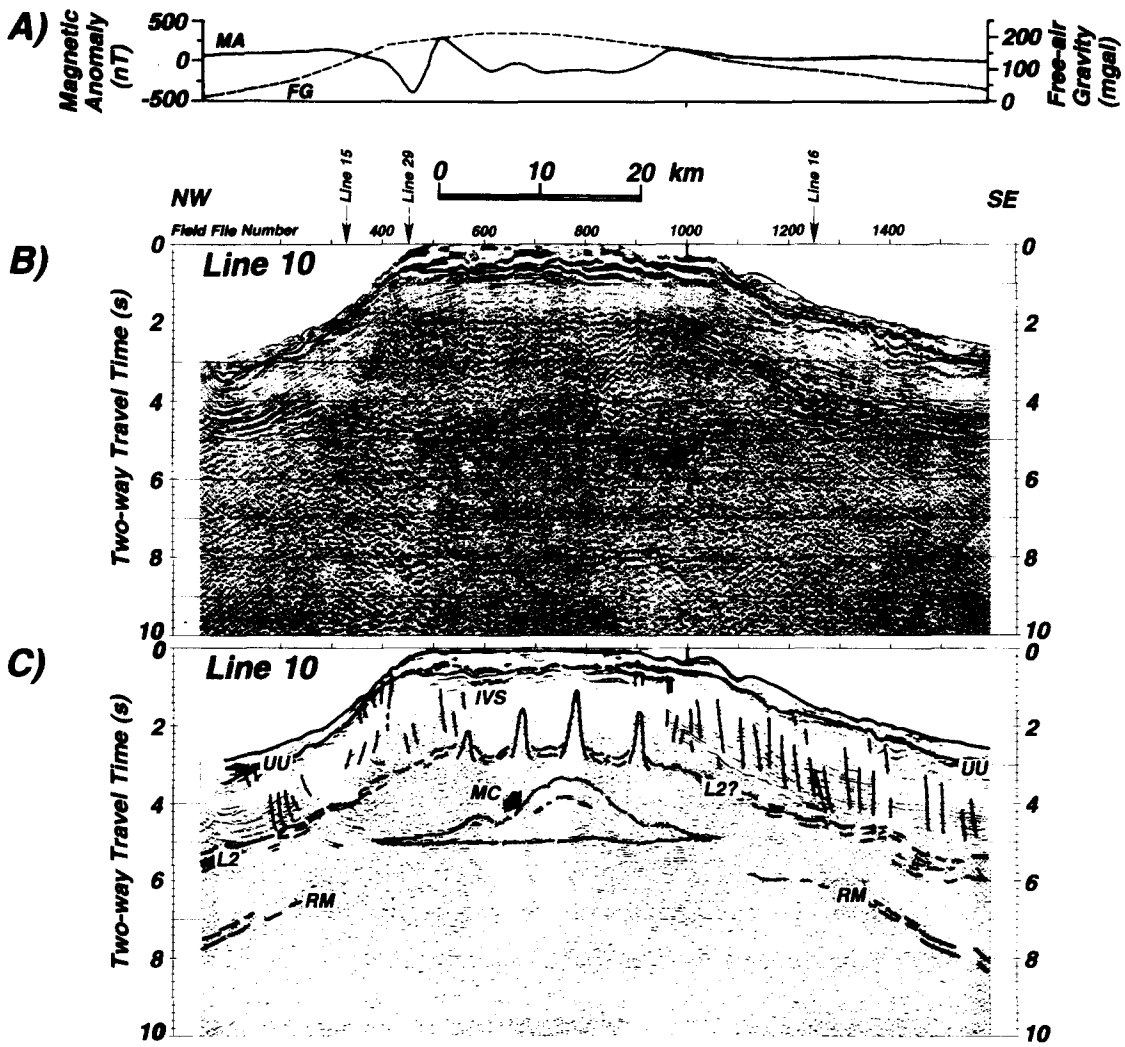

Fig. 4. WAPS deep-imaging MCS Line 10. (A) Free air gravity (FG) and magnetic anomaly (MA) profiles. (B) Migrated seismic section with a 2 s AGC window. Display is a positive polarity, variable area display, every third CMP trace. (C) Interpreted seismic section from (B). *RM* = reflection Moho; *L2* = top of oceanic basement layer 2; *MC* = magma chamber; *IVS* = intercalated volcanics and sediments; *UU* = uplift unconformity. Vertical to horizontal exaggerations for (B) and (C) were calculated using average interval velocities for the following crustal units: 5× for seafloor using a velocity of 1.5 km/s, 2× for bottom of sediment layer using a velocity of 3.5 km/s, 1× for crystalline basement using a velocity of 6.5 km/s, and 0.9× for crust–mantle boundary using a velocity of 8.0 km/s. See Fig. 1 for location and Section 3 for acquisition and processing parameters.

4.3. Crustal arching

Using gravity modelling, Hedberg (1969) proposed that CVL islands are underlain by thick sedimentary deposits overlying an oceanic basement. The WAPS MCS data confirm this interpretation (see also Meyers and Rosendahl, 1991), showing that CVL volcanic centers are not made up of thick piles of intraplate volcanic material like Hawaiian volcanic centers (cf. Watts et al., 1985). Instead, lava flows and related intrusives represent a cap less than 2 km thick overlying 4–5 km of pre- and syn-volcanic sediments (Figs. 2–4). These pre-volcanic sediments are probably a combination of distal turbidites, ranging in age from Aptian to Miocene, intermixed with pelagic sediments. The volcanic cap

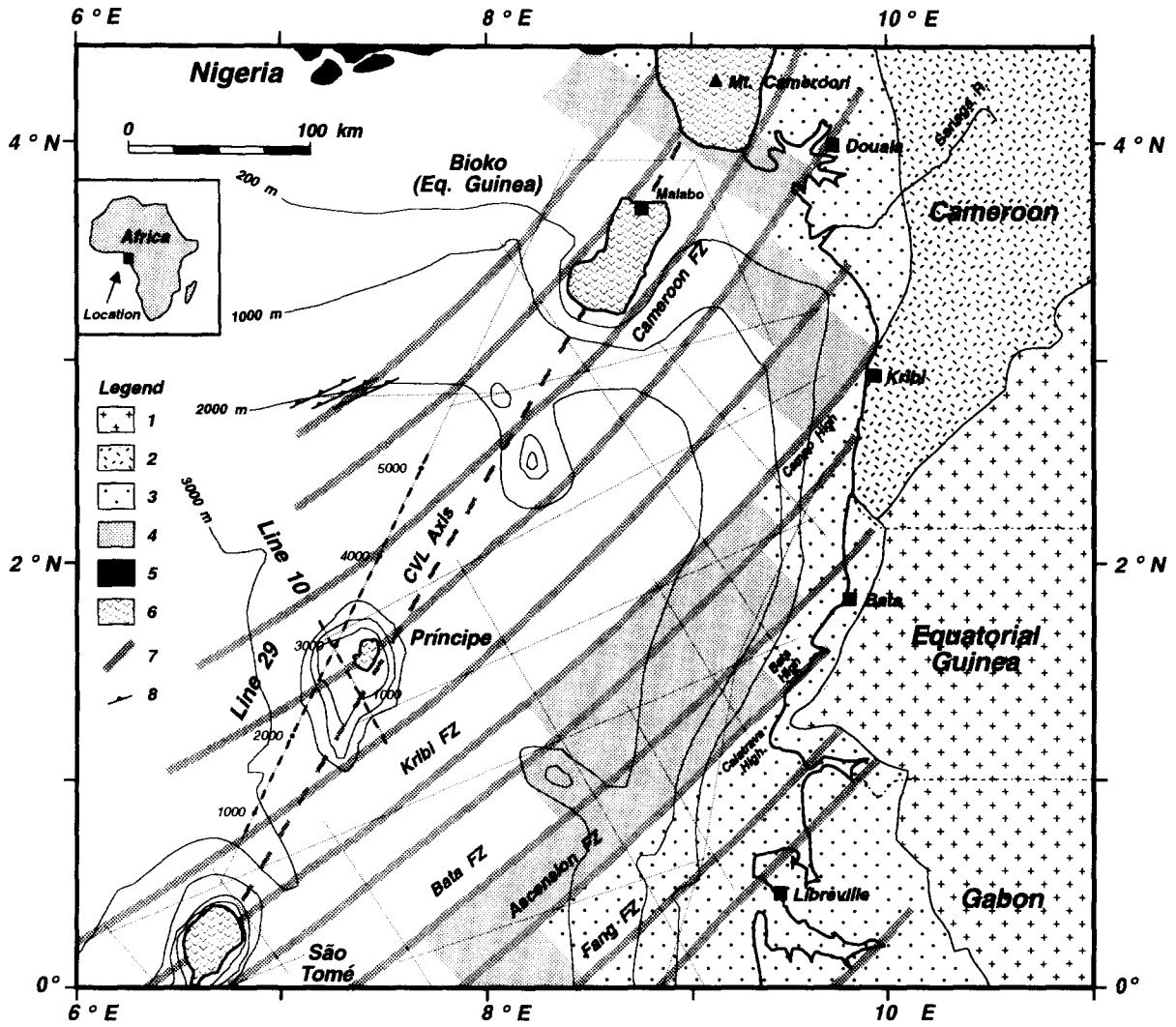

Fig. 5. Projected fracture zone crossings below the CVL adapted from Meyers et al. (1996). *1* = Archean Congo Craton; *2* = Late Proterozoic Pan African mobile belt; *3* = Mesozoic rifted continental crust; *4* = proto-oceanic crust in between rifted continental crust and 'normal' oceanic crust; *5* = subaerially exposed CVL volcanic rocks; *6* = onshore Tertiary Niger Delta sediments; *7* = transfer faults and oceanic fracture zones; *8* = Niger Delta toe thrusts. Plot is universal transverse mercator projection centered at 9°E.

is interpreted to represent the hummocky, moderately to highly reflective sequence occupying the interval from water bottom to 0.5 s two-way travel time (TWTT) below water bottom, between field files 1800 and 3800 on Line 29 (Fig. 3), and along the entire length of Line 10 (Fig. 4); note also the steep water bottom topography between field files 500–700 on Line 14 (Fig. 2). Stacking velocities from this volcanic-rich zone range between 3 and 4 km/s, which is ~1.5 km/s faster than horizontal reflector packages in the deep-water lows adjacent to the islands. These interpreted volcanic reflectors may be flows and sills intercalated with pre-volcanic and syn-volcanic sediments.

The main accumulation of intraplate volcanic rocks at CVL islands coincides with a regionally continuous unconformity of inferred Miocene age (UU, 'uplift unconformity', Figs. 2–4). Here, deep-water sedimentary reflectors have been uplifted below the flanks of CVL islands (see also Grunau

et al., 1975; Meyers and Rosendahl, 1991). The Miocene age for the uplift unconformity is obtained from correlation of this unconformity in sedimentary reflectors to offshore wells drilled north of Bioko [Fig. 1, Alba-1, 9A-1 and Bonito-1 (Hedberg, 1969) and 13-B-1X (Armstrong, 1985)], and from correlation of seismic reflections to WAPS well ties off Cameroon and Gabon. This uplift is not unique to Príncipe, as it also occurs at São Tomé, Bioko, the seamount between Bioko and Príncipe (Meyers and Rosendahl, 1991), and Pagalu (formerly Annobon) (Grunau et al., 1975).

Pre-uplift sedimentary and volcanic reflectors remain concordant in the zone of crustal uplift, but are difficult to trace through the axis of the crustal arch because of disruption by pervasive faulting and volcanism (Figs. 3 and 4). Hedberg (1969) has reported coarse-grained, lithic quartz arenites on São Tomé Island, and from lithology alone ascribed a possible Cretaceous age to these rocks. These sandstones may be pre-uplift deposits, but a Cretaceous age is highly tenuous. Miocene fossil assemblages are also reported in outcrops of pre-volcanic sediments on Príncipe Island, providing further evidence for Miocene crustal uplift (Delmas, 1982). Volcanic rocks on Príncipe have been dated to be as old as 30 Ma (Oligocene; Fitton and Dunlop, 1985; Halliday et al., 1988; Lee et al., 1994), but the period of crustal uplift is interpreted to have occurred during the Miocene, as shown by the uplift unconformity and uplifted, Miocene deep-water marine deposits on CVL islands and on the flank of Mt. Cameroon.

Crustal uplift also has caused the CVL to act as a structural barrier, separating sediment deposition in the Niger Delta/Rio Del Rey Basin from the Douala Basin since the Miocene (Fig. 1). Distal Niger Delta sediments younger than the uplift unconformity are ~1 s thick TWTT in saddles between crustal uplifts, and they lap onto sedimentary and volcanic reflectors that have been rotated by uplift along the Príncipe crustal arch (Fig. 3) and other CVL crustal uplifts (Meyers and Rosendahl, 1991). Sediments that onlap these crustal arches are considered here to be a combination of Miocene to Recent distal turbidites and volcaniclastic material derived from the CVL islands. Emery et al. (1975) reported that shallow water bryozoans, terrestrial plant material and coarse-grained sediments have been dredged in deep water along the Príncipe channel bordering the northwest side of the CVL (Fig. 1). Also, Gorini and Bryan (1976) refer to similarities between such adjacent deep-water sediment facies and uplifted sediments found on São Tomé Island.

Crustal uplift of CVL islands and seamounts appears to have been by gradual ramping or bending of the lithosphere, rather than by large vertical offsets along faults. Large vertical offsets are rare, and one exception is on Line 29 at field file 2500 (Fig. 3), where a zone of steep, normal faulting vertically offsets the crust by ~2 km over a horizontal distance of less than 5 km. The limb of the crustal arch forms a plateau southwest of this fault. The remainder of the crust adjacent to Príncipe Island appears to have been flexed upward only gently. This bending is presumed to have been accomplished by ductile creep from reheating of the lithosphere, as suggested for the continental potion of the CVL (Poudjom-Djomani et al., 1995), and small displacements along a large number of vertical faults. Such crustal reheating is probably responsible for modern heat flow values between CVL volcanic centers that are 16–34 mW/m^2 greater than surrounding oceanic crust, which has an average value of ~50 mW/m^2 (Herman et al., 1977; Wright and Louden, 1989).

4.4. Igneous intrusions

Some reflections below the shelf of Príncipe Island are interpreted to be from intrusive structures. Vertical chains of narrow diffraction hyperbolas, associated with small offsets and sediment piercement, cut across the sedimentary section throughout the crustal arch. Their frequency is greatest at the axis underlying the shelf of Príncipe Island (Figs. 3 and 4). These sub-vertical reflection features are interpreted to be mafic dikes and faults, and are only observed on the limbs of the volcanic arch, within 30 km of its axis (Figs. 3 and 4). The dikes appear to intrude along fractures, which may have accommodated normal shear associated with uplift. This implies a 'similar' style of folding to accommodate deformation of the entire upper crustal section, which was probably less ductile than the lower crust during reheating and uplift. The lack of large-scale extensional structures at the crest of the crustal arch supports this idea (Figs. 3 and 4). These fractures

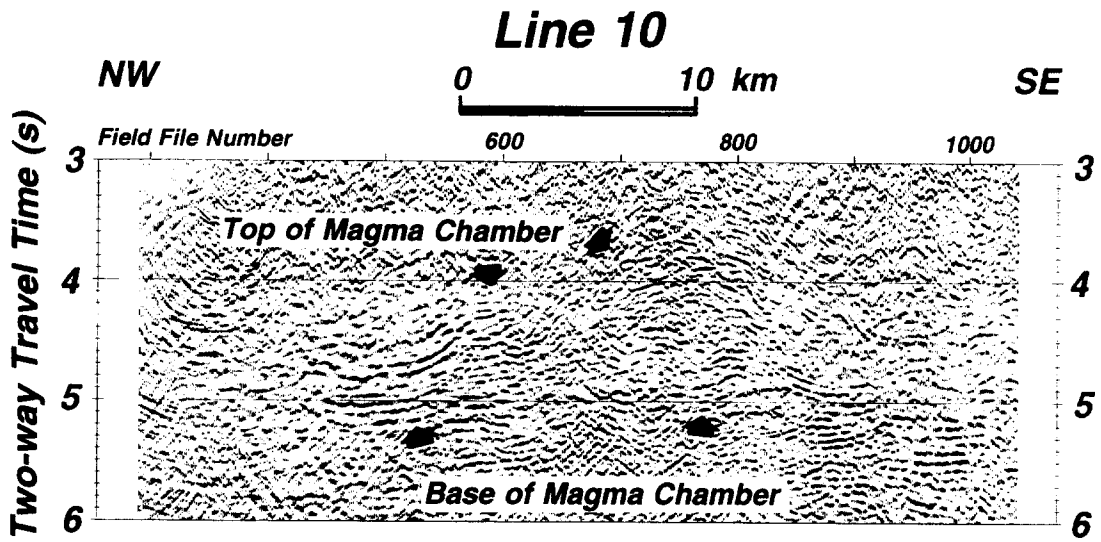

Fig. 6. Window of migrated MCS data from WAPS Line 10 (Fig. 2). Seismic section is plotted with a 2 s automatic gain control (AGC) window, positive polarity, variable area display, every third common mid-point (CMP) trace. This profile shows two dome-shaped reflective zones interpreted to be the tops of magma chambers or plutons that underlie the Príncipe shelf. A sub-horizontal band of reflectors that gently dip to the northwest occurs at 5 s TWTT, and is interpreted to be a cumulate horizon or weak reflection Moho. See Fig. 1 for location and Section 3 for acquisition and processing parameters.

also may accommodate any transcurrent shear along the CVL as proposed by Lameyre et al. (1984), as well as provide conduits for dykes and hydrocarbons[3]. These features may be similar to volcanic fissure eruptions observed trending northeast along the continental portion of the CVL (Fitton, 1983: Déruelle et al., 1987).

Below the shelf of Príncipe Island, domal reflections ~5 km wide are observed between 4 and 6 s TWTT (Fig. 3, field files 2700–3000; window in Fig. 6; Fig. 4, field files 600–900). These hyperbolic reflections occur within a zone that we interpret to be at or above Moho level. It is possible that these reflections are from the tops of magma chambers or plutons that may have cooled or are still in a ductile state from partial crystallization [seismic modelling indicates that reflections may be produced by zones of partial crystallization in magma chambers (Jacobs et al., 1992)]. Fig. 6 shows a window of MCS data from Line 10 that may outline a mafic batholith which has several domal tops. Multiple, arcuate reflections below the top of the interpreted plutons may be sideswipe from similar pluton structures laying outside the plane of the profile. This occurs on Line 29, which runs almost at right angles to Line 10 (Figs. 3 and 1). These domal reflection zones are floored by a weak band of sub-horizontal reflectors at ~5 s TWTT (Figs. 3, 4 and 6), which could mark the top of a cumulate horizon or a faint reflection Moho.

4.5. Gravity and magnetic data

Absence of high amplitude magnetic anomalies above oceanic crust adjacent to CVL crustal arches can be attributed to: (1) uniform, normally polarized remnant magnetization from formation of oceanic crust during the Cretaceous Quiet Period (cf. Sibuet and Mascle, 1978; Sclater et al., 1981; Scotese et al., 1988); and (2) submergence of oceanic crust beneath >2 km of seawater and burial by >4 km of sediments, so that basement highs, such as the Cameroon fracture zone, do not show strong fields at the sea surface.

[3] Volcanism at the Príncipe crustal arch probably caused maturation to overmaturation of organic accumulations in the sediments. Oil samples collected from seeps on São Tomé and Príncipe have API gravities of less than 30°, and a likely source for these oils are Albian to Turonian organic-rich shales deposited in an anoxic basin (cf. Tissot et al., 1980).

Relatively large amplitude anomalies in both free-air gravity and magnetics are associated with CVL crustal uplifts (Figs. 3 and 4). At the crest of the Príncipe crustal arch, magnetic anomalies are coincident with shallowing of oceanic basement and abundant Cenozoic volcanics that have probably erupted during times of both normal and reversed polarity (cf. Piper and Richardson, 1972). Free-air gravity increases over the crustal arch (Figs. 3 and 4). (Emery et al., 1975; see also map by Smith and Sandwell, 1997) first recognized that positive free-air anomalies are observed near CVL islands, but that an overall negative gravity anomaly surrounds the CVL swell. This negative gravity anomaly is approximately −40 mGal adjacent to the Príncipe crustal arch (Fig. 3). It is likely caused by a mass deficit in the upper mantle, as the lithosphere here does not appear to show downward flexuring adjacent to the uplift axis.

To model gravity, we have depth converted major crustal elements interpreted from interpreted MCS profiles using interval velocities from normal moveout (NMO) and average crustal and mantle velocities [adapted from Fowler (1992) and Allen and Allen (1990)]. The most reliable stacking velocity data down to Moho depths came from horizontal crust adjacent to crustal arches.

Across the axis of the CVL, seismic penetration was reduced by reflected energy from shallow igneous flows and scattering off irregular surfaces of these flows. In the CVL axis region, stacking velocities within the crust were further complicated by vertical igneous features and disruption of sub-horizontal reflectors by numerous, small offsets along sub-vertical faults. Depth conversion across the CVL axis was therefore made by correlating horizontal reflections from the flanks of the crustal arch through the axis, and taking into account increased velocity from igneous extrusives overlying interpreted sediment reflectors at the axis. The reflection Moho is observed to rise with uplifted crust below the flanks of Príncipe Island (Figs. 3 and 4), and for continuity in constructing a gravity model, we chose to continue the reflection Moho across the arch axis; although it was no longer seismically visible there (Fig. 7).

Density polygons were constructed from depth-converted crustal sections and modelled using a two dimensional method (Talwani et al., 1959). Crustal densities were assigned using values adopted from various gravity models presented in Fowler (1992) and Allen and Allen (1990). Gravity calculated using uncompensated, uplifted crustal sections and a zone of 'post-uplift' intercalated volcanics and sediments at the arch axis did not fit observed data. When a large polygon with a negative density contrast relative to surrounding mantle ($\Delta\rho = -0.1$ g/cm^3) was placed below crust affected by the Príncipe crustal arch, calculated gravity matched the observed gravity quite well (Fig. 7). Thus a NE-striking wedge of low-density mantle was chosen to compensate for sustained uplift of the Príncipe crustal arch. Such a large mass deficit below the CVL can explain an overall negative free-air gravity anomaly across the CVL, when the local mass attraction of islands is overlooked (Emery et al., 1975). This style of isostatic compensation differs dramatically from gravity models using compensating roots of mafic lower crust density (cf. Goslin and Sibuet, 1975; Detrick and Watts, 1979; Watts et al., 1985; Kellogg et al., 1987).

The mismatch of free-air gravity from calculated gravity near field file 2800 on Line 29 and at field file 700 on Line 10 (Fig. 7) may be due to increased mass associated with mafic intrusives. Hedberg (1969) has mapped an increasing gradient in Bouguer gravity anomaly of +4 mGal/km toward the southwestern corner of the island, and our data show a positive residual anomaly of ~15 mGal at the axis of the Príncipe shelf. This gravity trend may be caused by mass attraction of a mafic plug intruding sediments and the abundant dikes interpreted to occur at the center of the Príncipe shelf (e.g. Figs. 3, 4 and 6). A pair of Bouguer anomalies of similar magnitude underlie volcanic edifices on São Tomé, and Hedberg (1969) suggested that these anomalies were also caused by volcanic pipes.

5. Discussion

5.1. Crustal uplift along the CVL

WAPS MCS data show that the topographic expression of CVL islands and seamounts is produced by crustal uplift rather than by building of shield volcanos with thick crustal roots. These islands and seamounts are primarily composed of uplifted, old

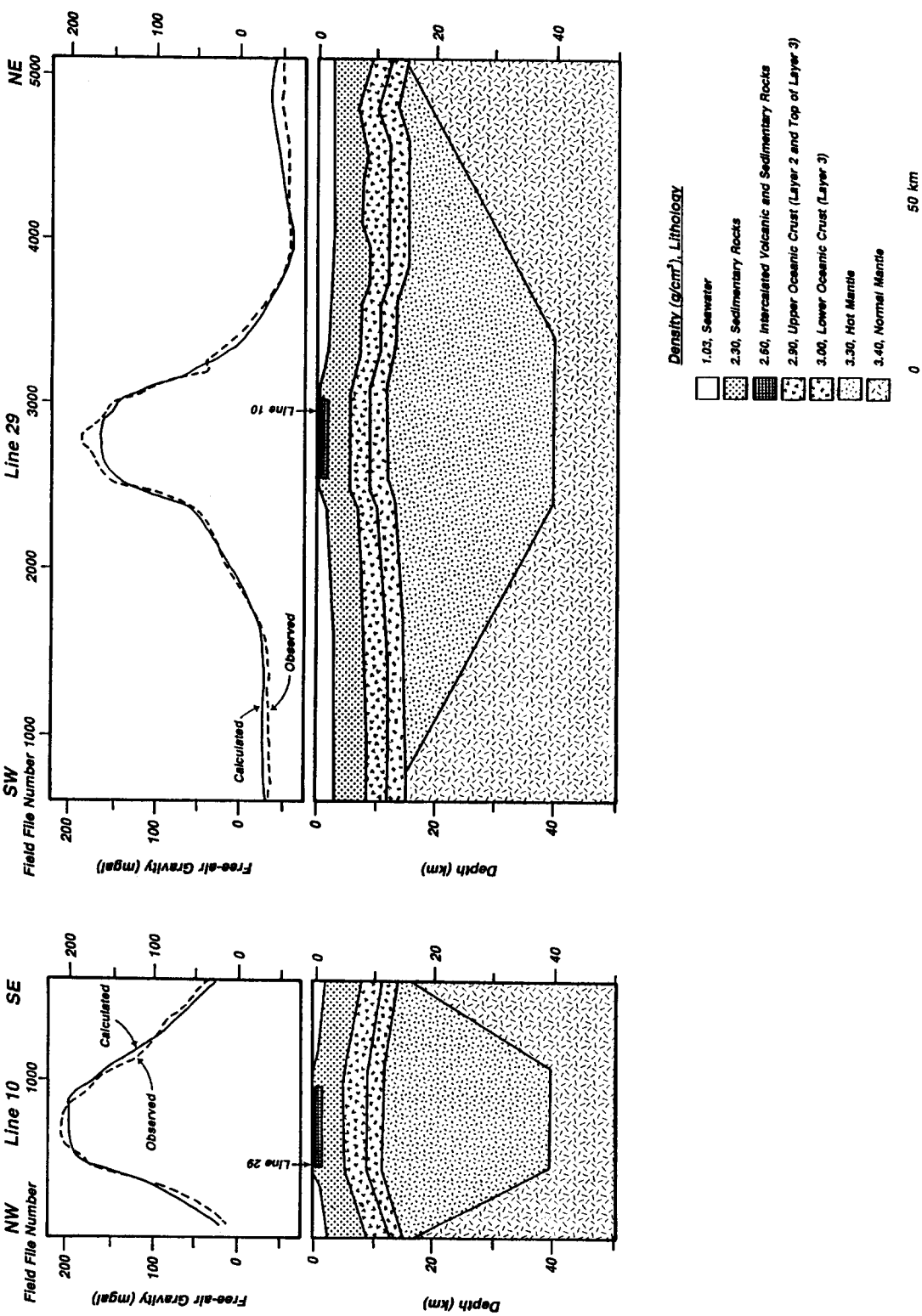

Fig. 7. Gravity model for WAPS lines 10 and 29. Interval velocities were calculated from root mean square velocities, and major crustal units were converted to depths and densities. Where velocity control was poor and there was no observable reflection Moho, calculated crustal thickness was projected through the axis of the crustal arch and some velocity assumptions were made. Gravity was modelled using a two-dimensional method from Talwani et al. (1959). Observed free-air gravity is dashed line and calculated free-air gravity is solid line. Note that the free-air gravity profile for the geologic model fits observed free-air gravity reasonably well using an inverted wedge shaped polygon with a mass deficit of -0.1 g/cm^3 below the uplifted crustal section. This mass deficit relative to surrounding mantle is suggested to represent a hot zone intruded by mafic material. Vertical to horizontal exaggeration is 2×.

oceanic basement (~110–90 Ma) and thick sediment cover, with a capping of volcanics extruded mainly during crustal uplift. The model in Fig. 8 shows how volcanism, crustal uplift and formation of the uplift unconformity may have evolved. Lack of flexural moats directly adjacent to volcanic centers is explained by the fact that the volcanic load is too small to overcome the elastic strength of the uplifted lithosphere, which may only be <20 km thick below the CVL (cf. Poudjom-Djomani et al., 1992, 1995). Such a thin lithosphere is in agreement with our proposal that oceanic crust was reheated during uplift to a point where upward bending overcame flexural rigidity along the CVL trend. The long wavelength gravity low across the CVL axis may, therefore, be caused by mafic partial melt intruding the mantle below the axis.

Shallowing of interpreted reflection Moho toward CVL islands may indicate that a low-density mantle underlies the crust. We have modelled this compensating mass as an elongate wedge of mantle material characterized by increased temperature and lower density, extending to a depth of 40 km (Fig. 7). This isostatic model also could represent a root of mafic underplating below the CVL. However, this idea is currently inconsistent with our suggested placement of reflection Moho at 1.7–2.5 s TWTT below the top of layer 2 at the flanks of the crustal uplifts (Figs. 3 and 4; Meyers and Rosendahl, 1991). Our model is exactly the opposite of what is observed at the Hawaiian volcanic chain, where gravity modelling and the reflection Moho below the hotspot trace indicates crustal underplating to compensate for the large intraplate volcanic pile (Watts et al., 1985).

Reheating of the lithosphere below the CVL to a depth of 40 km and resultant uplift of >3 km is consistent with observations over mid-plate swells (Crough, 1978, 1983). Reheating must be considered as a contributing factor to lower relative density, because modern heatflow values measured along the CVL are still considerably higher than in the sur-

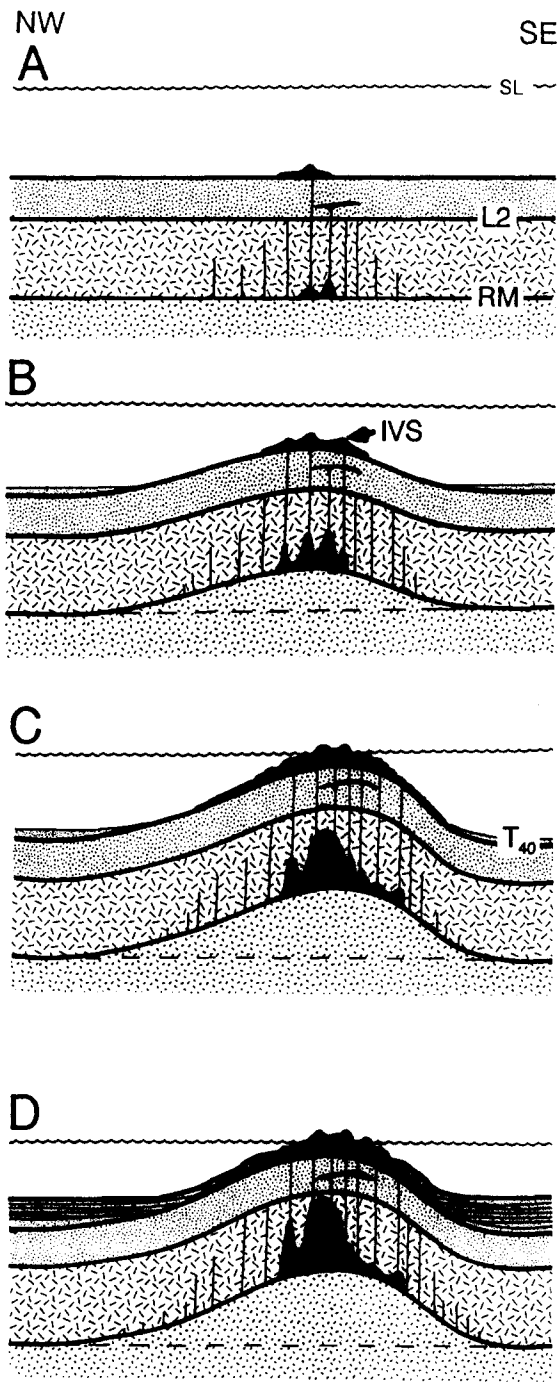

Fig. 8. Model showing evolution of crustal uplift across the CVL axis. (A) Submarine volcanism begins in the Oligocene (?). (B) Intrusion of mafic partial melt and reheating of mantle underlying the crust causes crustal uplift in the Early Miocene. (C) By Middle Miocene, uplift and volcanism are at their peak, and the uplift unconformity is created (T_{40}). (D) Modern profile of a crustal arch with sediments onlapping the uplift unconformity. *RM* = reflection Moho; *L2* = top of oceanic basement layer 2; *IVS* = intercalated volcanics and sediments.

rounding lithosphere (Herman et al., 1977; Wright and Louden, 1989). Along the CVL, reheating probably began in the Oligocene, possibly by some form of melt intrusion or convective transfer, followed by upward flexure of the lithosphere within a zone less than 200 km wide. Lack of noticeable subsidence, volcanism as young as the Pliocene, and high modern heatflow by themselves imply that mantle lithosphere below Príncipe has not cooled much since Miocene uplift.

A low density ($\Delta\rho = -0.05$ g/cm^3) zone of light mantle was modelled to have invaded the lower mantle lithosphere underlying the onshore portion of the CVL (Fairhead and Okereke, 1988; Okereke, 1988). Here, we have chosen to use a mass deficit of -0.1 g/cm^3 for a compensating body that directly underlies the uplifted crust. To account for such a density contrast purely by reheating of mantle peridotite, the relative temperature differences between the elongated wedge of hot mantle and surrounding rock would have to be +1225°C [$\rho_2 = \rho_1(1 - \Delta T\alpha)$, where $\rho_1 = 3.4$ g/cm^3, $\rho_2 = 3.3$ g/cm^3 and $\alpha = 2.4 \times 10^{-5}$ (volume coefficient of thermal expansion of peridotite); Allen and Allen, 1990; Fowler, 1992]. This relative temperature difference is unreasonably high, so too is the idea that the density contrast could only have been formed by conductive heat transfer (cf. Crough, 1983).

Another possible mechanism to produce our modelled low-density mantle wedge is intrusion by mafic partial melt derived from pressure-release during upwelling of the asthenosphere (cf. Detrick and Crough, 1978; Withjack, 1979; White and McKenzie, 1989). Basaltic pods, streaks and dikes are commonly found in mantle upwelling zones and in non-hotspot ophiolitic peridotites, especially in diapiric zones below inter-fracture zone highs along ridge crests (Nicolas, 1989; Downes, 1990). Mixed partial melt in mantle diapirs is believed to produce gravity lows on mid-ocean ridge crests (Lin et al., 1990), so it is not unreasonable to assume that this can occur under the CVL on a much larger scale.

Therefore, a mixture of residual mafic melt with mantle below the CVL may contribute to the negative density contrast. By mixing alone, a modelled density contrast of -0.1 g/cm^3 (lower density mantle wedge $\rho = 3.3$ g/cm^3) could be produced by combining cool lithosphere mantle ($\rho = 3.4$ g/cm^3) with 25% mafic melt ($\rho = 3.0$ g/cm^3). This idea considers only mixing of mafic and ultramafic rocks, but not elevated temperature of both the reheated mantle and mafic melt. Reality is probably somewhere in between reheating and addition of partial melt, because the CVL is still hot and volumetric addition of 25% mafic melt seems high.

Asthenospheric upwelling also may have contributed additional dynamic support to the CVL uplift. Columns of lithosphere adjacent to the Príncipe crustal arch and at the arch axis are not in exact isostatic equilibrium, according to our gravity model for Line 29 (Fig. 4). These columns take into account ~1.5 km of post-uplift sediment adjacent to the crustal arch and added density at the arch axis from volcanic material. This isostatic imbalance between columns comes out to be $+1.3 \times 10^6$ kg/m^2 for the Príncipe crustal arch, which amounts to 13% of observed uplift that is not fully compensated for by the modelled, hot mantle body in the lithosphere. Similar isostatic imbalances are found where columns of lithosphere above oceanic volcanic highs are compared to adjacent normal oceanic lithosphere, even though the density models fit observed gravity data (cf. Goslin and Sibuet, 1975; Watts et al., 1985; Kellogg et al., 1987). Ignoring flexural resistance to uplift, such isostatic imbalance can be explained only by an added component of dynamic uplift or elevated asthenospheric temperature (cf. Courtney and White, 1986; McNutt, 1988). Some component of dynamic uplift and reheating may still occur at the base of the lithosphere to prevent CVL crustal arches from subsiding and to maintain elevated heatflow (cf. Herman et al., 1977). In any case, the source for increased heating, mafic intrusions, and/or dynamic support must be within the sub-lithospheric mantle.

The lack of extensional structures and/or rift zones over crustal arches along the CVL argues against the idea of active rifting following thermal rejuvenation and uplift (cf. Bott and Kusznir, 1979; Bott, 1981; Keen, 1988; Okereke, 1988; Allen and Allen, 1990). Rifting may then be considered to be a passive rupturing of the lithosphere, and large igneous provinces associated with rifts may be created at zones of lithospheric tension coincident with mantle thermal anomalies (cf. White and McKenzie, 1989). Some may argue, however, that intraplate compressional stresses from the Alpine orogeny (cf.

Grunau et al., 1975) would have been parallel to NW–SE-oriented extensional stress fields, thus preventing rift development.

WAPS MCS profiles also show that crustal uplift perpendicular to the CVL trend is asymmetric, with a gentle ramp on the northwest side and a steeper southeast side (Meyers and Rosendahl, 1991). Uplift asymmetry could be explained by intraplate compression from the collision between the African and Eurasian plates during the Miocene, but compression does not fit with coeval volcanism along the CVL, and the collisional zone may be too far away. Aside from horizontal, intraplate compressive stresses, asymmetrical uplift across the CVL can be explained by differential vertical stresses, subtle northward drag of the African plate over a fixed zone of upwelling (see Gripp and Gordon, 1990), or a SE-directed shift of a mantle upwelling zone over a fixed plate.

5.2. *Volcano spacing*

In addition to the lithosphere being weakened by reheating, uplifted volcanic centers may coincide to fracture zone crossings. Fracture zones have been mapped using WAPS data to cross the CVL and then veer more northeast to the east of the CVL (Fig. 5; Meyers et al., 1996). In most cases, the large volcanic uplifts are coincident with these preexisting weakness zones, as originally proposed by Vogt (1974). For example, the large normal fault zone on Line 29 at field file 2500 (Fig. 3) may represent rupture along a preexisting fracture zone crossing that was reactivated during uplift of the footwall block. It must be noted, however, that the strike of this fault is indeterminate with present seismic coverage, and it may strike to the northeast, paralleling bathymetric contours (Fig. 5).

The seamount between the islands of Bioko and Príncipe is also a zone of crustal uplift (Fig. 2; Meyers and Rosendahl, 1991). This seamount overlies the proposed crossing by the Cameroon Fracture Zone through the CVL, before it turns northeast into the African mainland, just south of Mt. Cameroon (Fig. 5). A concentrated zone of seismicity occurs in the uppermost mantle southeast of Mt. Cameroon (Ambeh et al., 1989; Ambeh and Fairhead, 1991), corresponding to the location where we have projected the onshore extension of the Cameroon Fracture Zone. However, because the distance between fracture zones in this region is small and their frequency is high, the correlation of volcanic centers to fracture zone crossings may be fortuitous.

Although volcanic centers appear to develop over fracture zone crossings in the oceanic portion of the CVL, the spacing of volcanic centers along the onshore portion of the CVL cannot be explained by this relationship. Moreau et al. (1987) mapped en échelon fault and lineament orientations along the landward portion of the CVL, and used autocorrelation analyses to show that these fault/lineament patterns were produced by sinistral transcurrent shear oriented 030°NE. Déruelle et al. (1987) mapped similar trending faults on Mt. Cameroon, which is also elongated along a 030°NE trend, and they asserted that Mt. Cameroon formed above tension gashes produced by sinistral shear along the Adamawa and Foumban shear zones.

The suggestion by Moreau et al. (1987) that the CVL may be a product of en échelon tension gashes related to sinistral transcurrent shear is also possible. The 200 m isobaths of São Tomé and Príncipe Islands show that they form rhomb-like shapes and are almost identical in size (Fig. 1). One set of sides trends roughly parallel to fracture zones and the other set trends roughly due north (Fig. 5). The long diagonal of both rhomb-shaped island pedestals trends roughly parallel to the CVL axis. The orientation of these structures may result from N–S-directed principal horizontal stress, which also would create sinistral shearing along the CVL axis. Faults on the CVL islands parallel sides of the rhombs and trend northeast and northwest (Hedberg, 1969). Dike swarms on Príncipe Island also trend northeast (Fitton, 1983). These dykes may then follow vertical Mohr–Coulomb failure plains within the islands.

The inferred transcurrent motions along the CVL may be related to intraplate stresses that are released along zones of weakened lithosphere. Such 'translithospheric gashes' (Lameyre et al., 1984) may help to explain volcanic crater spacing, along with preexisting weakness zones, but CVL magmas and uplift must originate from below the lithosphere.

Another explanation for the spacing of volcanic centers independent of fracture zones or shearing may relate to the geometric nature of magma pen-

etrating the lithosphere from an underlying, linear zone of hot mantle or 'hotline'. Models used to describe spacing of magma chambers along spreading ridges show that Rayleigh–Taylor instability may develop undulations that give rise to discrete diapirs at regularly spaced intervals (Nicolas, 1989; Lin et al., 1990; Schouten and Whitehead, 1991–1992). Below the CVL, similar upwelling of regularly spaced diapirs, but on a larger scale, is conceivable if the existence of a linear zone of hot asthenosphere is accepted as the source for this line of diapirs (see also Rohrman and Van der Beek, 1996).

5.3. CVL/St. Helena hotline

Similar geochemistries of basalts from oceanic and continental portions of the CVL has led Fitton and Dunlop (1985) to theorize that a sub-lithosphere upper mantle source is responsible for volcanism that lasted 65 Ma along the CVL. Cantagrel et al. (1978) have found lower Tertiary alkali ring complexes (granite, syenite, gabbro, ca. 66–30 Ma) from the CVL to be similar to those found >200 km northwest of the CVL axis in Nigeria. It is likely that this older phase of plutonism in the landward portion of the CVL is unrelated to younger alkali basaltic volcanism, and may have resulted from transcurrent tectonism associated with reactivation along the Benue Trough and the Central African shear zone (cf. Fairhead, 1988; Benkhelil, 1989; Fairhead and Binks, 1991; Binks and Fairhead, 1992).

On the Seasat gravity anomaly map of Haxby (1987) and combined Geosat and ERS-1 gravity map of Smith and Sandwell (1997), a chain of seamounts appears to continue southwest from CVL islands to St. Helena Island, ~800 km east of the Mid-Atlantic Ridge (Fig. 1). St. Helena is a Miocene volcanic island (Baker et al., 1967; Baker, 1973) located on Eocene oceanic crust (Rabinowitz and LaBrecque, 1979). Many authors believe that St. Helena Island overlies a hotspot that is responsible for creation of the entire CVL, and so hence believe it is part of the CVL (Morgan, 1972, 1983; Duncan and Richards, 1991; O'Connor and Le Roex, 1992; Wilson, 1992). We propose that the main building phase of St. Helena Island was coeval with crustal uplift and volcanism described for CVL volcanic centers to the northeast. Crustal uplift has not been documented at St. Helena Island, but it has not been suspected and therefore not tested. Based on St. Helena's age and occurrence on the CVL bathometric trend, we postulate that it formed over the southwest end of the hotline underlying the CVL. If the entire CVL had its main uplift and volcanic phase in the Miocene, uplifted seamounts should not occur on oceanic crust younger than Miocene to the southwest of St. Helena Island.

A low S-wave velocity anomaly, characteristic of a plume head, has been described to underlie the lithosphere at St. Helena, and a low-velocity channel extending westward is thought to be caused by asthenosphere flowing from this plume head toward the nearby Mid-Atlantic Ridge (Zhang and Tanimoto, 1992). This low-velocity channel could also represent the SW termination of a hotline, but the poor resolution of seismic tomography in this region must be taken into account.

6. Similarities between the CVL and other Eastern Atlantic volcanic island chains

The seismic expression of the CVL uplift unconformity is similar to unconformities found at other intraplate volcanic chains in the Eastern Atlantic that have undergone a profuse phase of alkali-rich volcanism peaking in the Miocene (Fig. 9). Islands in these other chains often contain exposures of pre-volcanic sediments and they do not have flexural moats surrounding volcanic highs, because they are predominantly comprised of uplifted oceanic crust, or they are suspected to have formed coeval to adjacent oceanic lithosphere. All volcanic island chains off of West Africa seem to show intraplate volcanic activity beginning in the Oligocene and peaking in the Miocene, they appear to form linear trends crossing fracture zones at oblique angles, they still have anomalously high heatflow values (Francheteau and Le Pichon, 1972; Burke and Wilson, 1972; Emery et al., 1975; Herman et al., 1977; Lancelot and Seibold, 1978), and they overlie elongate negative depth anomalies (actual depth–depth predicted by age depth curve, Crough, 1983). Although some of these volcanic islands and seamounts may have been produced by time transgressive volcanism over hotspots, they all share a common feature: basement uplift exceeding 1 km. Structural architecture of this

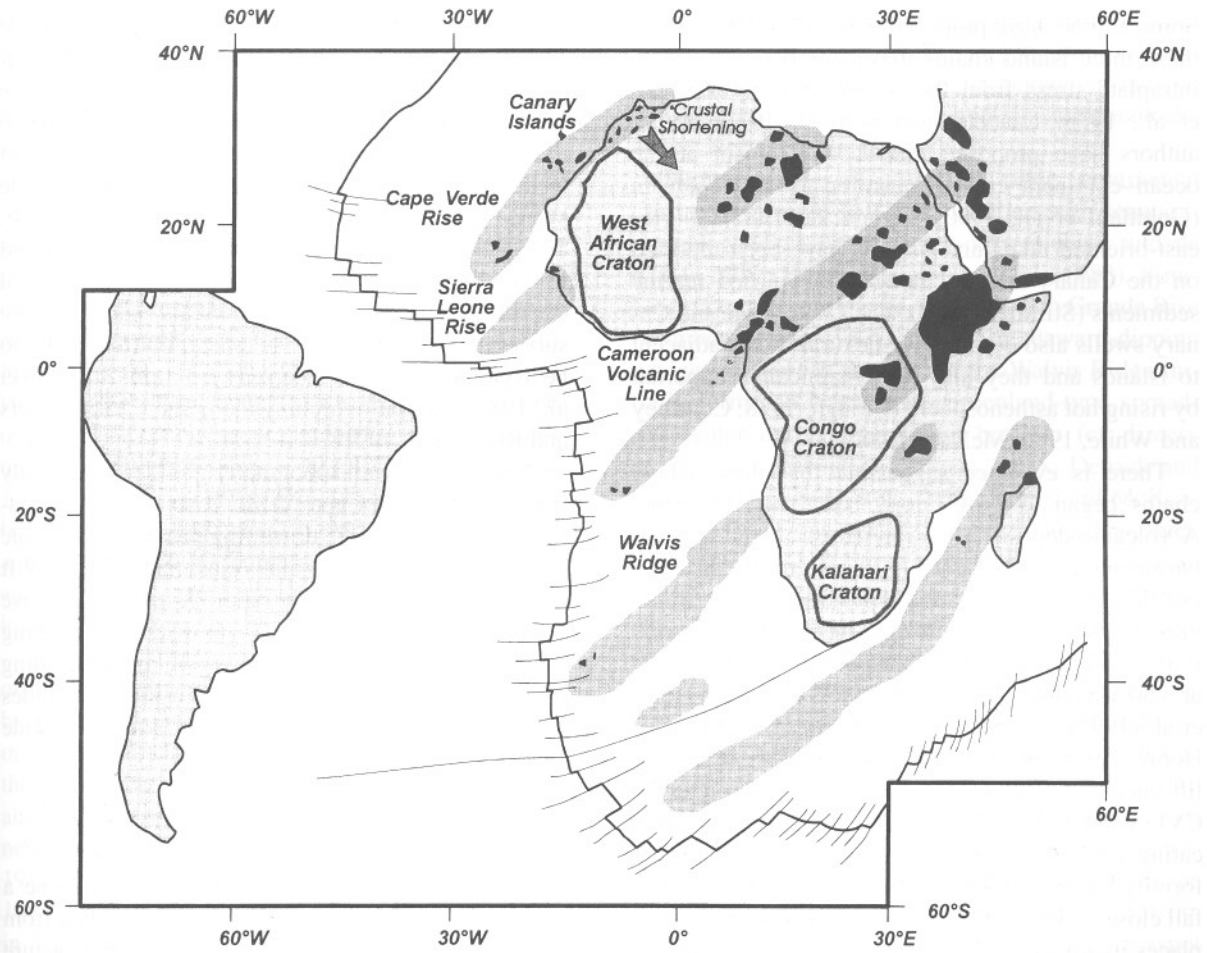

Fig. 9. Projected hotlines beneath the African plate. Solid black areas are subaerial exposures of Neogene intra-plate volcanic rocks. Zones of Neogene volcanism on the African continent and offshore are shaded to show the location of hotlines. Gaps in volcanism occur at Archean cratons, which are considered to be underlain by deep lithospheric roots. The more easterly trend of the hotline to the east of the Canary Islands may be caused by crustal shortening at the collision zone between African and Eurasian plates. Spacing of these hotlines may be produced by upper mantle, Rayleigh–Benard convection (see text and Fig. 10). Plot is mercator projection tangent at the equator.

style of uplift sets Atlantic volcanic chains apart from classical Hawaiian-type volcanic lineaments which are comprised of thick piles of intraplate volcanics that locally produce downward flexure at the crest of a broad swell.

6.1. Canary and Cape Verde islands

Synchronous volcanic episodes and uplift of originally horizontal sediments has been shown to have occurred during the Miocene at the CVL, Canary Islands and Cape Verde Islands (Grunau et al., 1975). Well-documented exposures of thick, Mesozoic deep-water sediments on the Canary and Cape Verde Islands are evidence of their uplift (Hedberg, 1969; Grunau et al., 1975; Stillman et al., 1982; Robertson and Bernoulli, 1982; Stillman, 1987; Rothe, 1990). Syn-volcanic sediments give Miocene ages for initiation of uplift (Lehner and de Ruiter, 1977; Lancelot and Seibold, 1978; Robertson and Bernoulli, 1982; Rothe, 1990). Drilling by the DSDP has also documented increased volcanism accompanied by uplift of oceanic basement in the Miocene for these island chains (Lancelot and Seibold, 1978).

Some authors have proposed that crustal uplift along these three island chains may have been related to intraplate stress from the Alpine orogeny (Grunau et al., 1975; Lancelot and Seibold, 1978). Other authors have proposed renewed volcanism at the ocean–continent crustal transition as a mechanism (Goldflam et al., 1980; Schmincke, 1982). Northeast-oriented dikes and fissures have been reported on the Canary Islands, along with uplifted marine sediments (Stillman, 1987). The Cape Verde and Canary swells also do not have flexural moats adjacent to islands and they may be dynamically supported by rising hot asthenosphere (Crough, 1978; Courtney and White, 1986; McNutt, 1988).

There is evidence suggesting that these island chains began to evolve long before the Miocene. A volcanic deposit is interpreted to overlie oceanic basement and sediments northeast of the Canary chain, and that this deposit appears to be time transgressive toward the southwest, indicating migration of the African plate over a hotspot that became active at ~60 Ma (Holik et al., 1991). MCS data from Holik et al. (1991), along with other studies (Watkins and Hoppe, 1978; Goldflam et al., 1980), show an uplift unconformity, similar to the one observed at the CVL, except that onlapping sediments fan out, indicating syn-sedimentary uplift. However, this unconformity has been interpreted by Holik et al. (1991) to fall close to the Cretaceous/Tertiary boundary, which places its time of formation long before CVL uplift. Yet, structural observations of Holik et al. (1991) show the Canary chain differs from Hawaiian-type hotspots, because they document sustained basement uplift, and their volcanic unit represents a relatively small volume of extrusives. The hypothesis of Holik et al. (1991) also involves increased volcanism and uplift continuing long after initial plume head and lithosphere interaction at ~40 Ma.

A conspicuous Miocene uplift unconformity has been identified on the western flank of Conception Island bank in the Canary Islands (Goldflam et al., 1980). Ages of the southwestern Canary Islands (Schmincke, 1982), however, could loosely fit SW-directed progression of a Canary hotspot on the African plate, as predicted by the model of Holik et al. (1991).

The Cape Verde Islands show the same type of structural features as the Canary chain and CVL, and there is no clearly documented evidence for systematic time transgressive, lateral volcanism, as would be expected for a hotspot trace. This has been reconciled by considering its location to be close to the rotation pole of the African plate with respect to the hotspot presumed to underlie the Cape Verde swell (Morgan, 1972, 1983; Duncan and Richards, 1991; O'Connor and Le Roex, 1992). Maio Island in the Cape Verde chain is made up of uplifted oceanic basement, marine sediments, and Neogene subaerial, alkali basalts. The crustal uplift appears to be asymmetric, with a steep eastern limb (Stillman et al., 1982), similar to arching along the CVL (Meyers and Rosendahl, 1991).

Analysis of swell topography and geoid anomaly suggests that the Cape Verde Rise overlies a stationary zone of mantle upwelling providing dynamic support as well as thermal rejuvenation for uplift (McNutt, 1988). Courtney and White (1986) have chosen to model the Cape Verde Rise as overlying a mushroom-shaped, convective plume emanating from the 650 km discontinuity. Their model includes downwelling zones enveloping this 1500 km wide zone of fountain-like upwelling.

6.2. *Sierra Leone Rise*

The Sierra Leone Rise has been shown to be a broad, NE-striking aseismic ridge that extends from the West African margin to the St. Paul Fracture Zone (Fig. 9). It may be composed of high-velocity volcanic material and deep crustal rocks (Sheridan et al., 1969; Emery et al., 1975; Sibuet and Mascle, 1978). DSDP sites 366 and 366A showed uplifted and rotated sediments over the rise and a depositional hiatus in the Miocene, which is thought to be related to a rise in the carbonate compensation depth or scouring by deep currents (Lancelot and Seibold, 1978). If uplift occurred in the Miocene, the rise would have been susceptible to slumping, erosion and reworking by currents over this feature.

The Sierra Leone Rise is similar to the CVL in having steeper slopes on its southeast side and having onlapping sedimentary reflectors that indicate tectonic uplift has occurred (Hedberg, 1969; Emery et al., 1975; Lancelot and Seibold, 1978). Also, Miocene volcanism has been described along the coast of Senegal (Lo et al., 1992), and may be

related to continuation of the Sierra Leone Rise to the northeast.

6.3. Walvis Ridge

The Walvis Ridge also has striking similarities in trend, width and length to the CVL (cf. Morgan, 1972; Francheteau and Le Pichon, 1972; Emery et al., 1975; Herman et al., 1977; Van der Linden, 1980; Morgan, 1983; Haxby, 1987; Duncan and Richards, 1991; O'Connor and Le Roex, 1992). Some of the relief along the Walvis Ridge was initially attributed to Cenozoic crustal uplift along lines of crustal weakness accompanied by volcanism (Ewing et al., 1966; Goslin et al., 1974; Emery et al., 1975). The Walvis Ridge also has been considered to be a long-lived hotspot trace (Morgan, 1972; Goslin and Sibuet, 1975; O'Connor and Duncan, 1990), but again there are some peculiarities that do not fit the hotspot paradigm.

In the northeast, the ridge is likely composed of detached slivers of continental basement formed by dual seafloor-spreading (Van der Linden, 1980) or westward ridge jump (Sibuet et al., 1983) in the Early Cretaceous. The northern flank forms an abrupt scarp and appears to be composed of continental crust (Goslin et al., 1974; Goslin and Sibuet, 1975; Van der Linden, 1980; Musgrove and Austin, 1984; Sibuet et al., 1984). The abrupt transition in crustal thickness across the northern end of the ridge has been interpreted to be a fault (Francheteau and Le Pichon, 1972; Musgrove and Austin, 1984), which may represent a protruding fracture zone margin (Francheteau and Le Pichon, 1972; Van der Linden, 1980). (Musgrove and Austin, 1984, their fig. 7, seismic unit 3) show onlap of what appears to be upwardly tilted reflectors by Miocene sediments toward this fault. This large vertical fault could have been reactivated during tectonic uplift, thus forming the Miocene unconformity. Miocene volcanic rocks also have been reported where this fracture zone reaches the West African mainland (Francheteau and Le Pichon, 1972).

Also in the northeastern portion of the ridge, an apparent uplift unconformity can be found on the southern flank (Goslin et al., 1974, their figs. 6 and 7; Goslin and Sibuet, 1975, their lines 2 and 9). This unconformity is remarkably similar to the uplift unconformity adjacent to CVL crustal uplifts. Such uplift suggests that there is more to the idea that the ridge formed solely by contemporaneous hotspot volcanism or foundering of continental crustal blocks during early seafloor spreading.

Further southwest along the ridge, continental crust gives way to half-grabens filled with seaward-dipping wedges of volcanic rocks (Lehner and de Ruiter, 1977; Hinz, 1981; Sibuet et al., 1983). Similar structures occur on the conjugate Rio Grande Rise (Gamboa et al., 1983), and these seaward-dipping wedges may prove that part of the Walvis Ridge initially formed a Norwegian–Greenland-type spreading center during continental breakup (cf. Emery et al., 1975; Goslin and Sibuet, 1975; Detrick and Watts, 1979; Sibuet et al., 1984; White and McKenzie, 1989; O'Connor and Duncan, 1990). This thick volcanic crust is believed to be underlain by a compensating crustal root reaching 25 km into the mantle and producing isostatic equilibrium without flexural deformation (Goslin and Sibuet, 1975; Detrick and Watts, 1979). Creation of this crust then likely occurred in proximity to the proto-Mid-Atlantic Ridge and is in agreement with dates of Walvis Ridge volcanic rocks semi-coincident with the age of adjacent oceanic basement (Goslin and Sibuet, 1975; Detrick and Watts, 1979). Goslin and Sibuet (1975) and Detrick and Watts (1979) also proposed that the Mid-Atlantic Ridge migrated westward, away from a fixed hotspot at ~80–70 Ma, and this hotspot then continued to produce volcanic seamounts in the southwestern portion of the Walvis Ridge.

Volcanism along the southwestern portion of the ridge appears to be restricted to narrow zones, as the ridge grades into elevated oceanic basement and seamounts. Here the ridge is asymmetrically steeper on its SE side and is mantled by uplifted Tertiary sediments (Ewing et al., 1966; Goslin et al., 1974; Emery et al., 1975; Goslin and Sibuet, 1975; Detrick and Watts, 1979), similar to other Atlantic volcanic island chains mentioned here. The volcanic highs form an en échelon pattern stepping to the southwest, and seem to coincide with fracture zone crossings, indicating that volcanism post-dates creation of oceanic crust (Goslin et al., 1974; Van der Linden, 1980). The southwestern portion of the ridge does not behave like a hotspot trace, because its topographic relief does not increase towards the SW,

where heating and volcanism is supposed to be the youngest (Van der Linden, 1980), and the ridge is still has elevated heatflow along most of its length (Herman et al., 1977).

7. African plate hotlines and upper mantle convection

7.1. African plate hotlines

In light of our interpretations of WAPS deep-imaging MCS data from the oceanic portion of the CVL, an alternative model to the hotspot idea is proposed. These data clearly show uplift of oceanic crust and pre-Miocene sediments, and volcanism to be contemporaneous between islands and seamounts. This architecture raises questions as to the nature of the CVL and other West African volcanic chains that show similar structures.

Linear depth anomalies and crustal uplifts with associated Neogene volcanism in the eastern Atlantic ocean have parallel trends and spacings between 1500 and 1800 km (Fig. 9). Parallel, NE trends and apparent age progressions of volcanism along these swells have been used to construct absolute poles of rotation for the African Plate with respect to relatively fixed hotspots thought to underlie these swells (Morgan, 1972, 1983; Duncan and Richards, 1991; O'Connor and Le Roex, 1992). Yet, Morgan (1983) has readily admitted there was a lack of consistent age progressions for most of these inferred hotspot tracks.

We provide an alternative hypothesis to the hotspot concept. Northeast-trending volcanic chains off the West African margin are manifestations of linear upwelling zones of hot mantle, 'hotlines', that produced crustal uplift and intraplate volcanism during the Miocene. The average parallel separation of these inferred hotlines is ~1700 km, which gives a half-width of ~850 km. This separation is similar to modelled upper mantle convection cells, where elongated zones of rising hot mantle are evenly separated by elongated zones of sinking cooled mantle (McKenzie, 1983). This style of upper mantle convection is thought to take place above the 670 km discontinuity, where an increase in S-wave velocity is believed to coincide with solid phase transformations from spinel to perovskite and magnesium oxide (McKenzie, 1983; Allen and Allen, 1990; Davies and Richards, 1992; Ita and Stixrude, 1992).

Vogt (1991) proposed a similar model of paired, linear zones of upper mantle convection coupled to the lithosphere for the Bermuda Rise and western flank of the Appalachian fold belt. Zones of upwelling are spaced ~1700 km apart and are separated in the middle by downwelling zones. He explained these zones as likely products of either intraplate stress during episodes of plate reorganizations or long-lived zones of asthenospheric convection coupled to the lithosphere. The hotline hypothesis also may be used to explain linear chains of coeval intraplate volcanism and domal uplift in this region (cf. Jansa and Pe-Piper, 1988).

7.2. Hypothesis on upper mantle convection mechanism

Small-scale convective rolls have been thought to develop within plate interiors, far from active plate boundaries. Such convective rolls involve two-scale convective flow in the upper mantle; one involving ridges and trenches below plate boundaries, and the other involving small-scale flow to produce upwelling and downwelling flow along cylindrical Rayleigh–Bernard convection cells with diameters of 650–700 km (Richter, 1973; Richter and Parsons, 1975). These smaller scale convective cells have been considered to be a mechanism for heat transfer to the base of the lithosphere and to mix upper mantle material (Richter, 1973; Richter and Parsons, 1975; Herman et al., 1977).

Richter and Parsons (1975) modelled linear convective rolls produced by shear along the lithosphere–asthenosphere boundary, parallel to the direction of fast moving plates (velocities >10 cm/yr), as in the Pacific Ocean. Such fast moving plate motions were modelled to produce cylindrical, upper mantle convective rolls with axes oriented parallel to the spreading direction (longitudinal rolls) within a 20–50 Myr time span after initiation of fast spreading (Richter, 1973). In the model, these elongated rolls had opposing rotation directions, which produced linear zones of alternating upwelling and downwelling between these rolls. This type of convection in the upper mantle would involve flow at Rayleigh numbers on the order of 10^5–10^6, but is

sensitive to perturbations and would become unstable at higher Rayleigh numbers. These convective rolls also were modelled to have secondary flow in the direction of their long axes.

Marsh and Marsh (1976) tested this hypothesis by processing global gravity data to isolate anomalies that may be produced by longitudinal rolls. Anomaly wavelengths of low degree and order of field 12 and lower were subtracted from a field complete to the 22nd order. The map of the processed data (Marsh and Marsh, 1976, their fig. 5) showed E–W and WNW-striking gravity lineations in the Pacific Ocean, with amplitudes of ~30 mGal and trough-to-peak separations of ~1000 km. These authors considered the gravity anomalies to be caused by longitudinal convective rolls that returned flow at a depth of 925 km, with aspect ratios close to 1. Separations of 1000 km, that involve convection above the 670 km discontinuity would require aspect ratios of ~1.8, which is still within reason given viscosity stratification at the 670 km discontinuity, and small amounts of internal heating (Marsh and Marsh, 1976; McKenzie, 1983). Longitudinal rolls also were used to explain non-time transgressive intraplate volcanism, with basalt containing high $^{87}Sr/^{86}Sr$ and $^{206}Pb/^{204}Pb$ ratios along the Easter volcanic chain in the southeastern Pacific Ocean (Bonatti and Harrison, 1976; Bonatti et al., 1977). These studies were later supported by Baudry and Kroenke (1991), who imaged parallel geoidal anomalies in filtered Seasat data. They also attributed these anomalies to longitudinal convection rolls in the upper mantle.

For slower spreading ridges, ~2.5 cm/yr, initiation of longitudinal rolls from shear at the lithosphere–asthenosphere boundary could take a minimum of 200 Ma to get established (Richter and Parsons, 1975). This is much too long for Atlantic hotlines off West Africa to have been developed from this mechanism, and depth anomalies associated with West African hotlines do not parallel oceanic flow lines, except where volcanics issue through old oceanic fracture zones or were emplaced near the ridge axis. Still, Herman et al. (1977) hypothesized that linear volcanic chains in the South Atlantic were not hotspot traces, but hotlines that formed by shear at the lithosphere–asthenosphere boundary that was not oriented parallel to flow lines. This hypothesis helped to explain the volcanic line spacing and elevated heatflow along the lengths of these volcanic island chains.

We use the models of Richter (1973) and Richter and Parsons (1975) to describe qualitatively the formation of inferred hotlines off West Africa. We propose a variation of their model, which involves little-to-no initial shear at the upper boundary layer, the lithosphere–asthenosphere boundary, and a high degree of unidirectional shear at the lower boundary layer, the 670 km discontinuity. This reverses the boundary layers in their model, relies on having sufficient friction at the 670 km discontinuity, and a mantle viscosity contrast which increases by an order of magnitude into the lower mantle (Davies and Richards, 1992). This idea also implies that African Plate volcanic centres that were active throughout the Neogene should have remained stationary. This is supported by the fact that such volcanic centres are documented to have remained in their current locations since the early Miocene (Burke and Wilson, 1972).

Velocities of mantle flow seem to be on the same scale as fast-moving plates and shear stress at the 670 km discontinuity is consistent with models involving a two layer convecting mantle (Davies and Richards, 1992); although the degree of shear depends on viscosity contrasts across this boundary. Lateral deflection of descending lithospheric slabs at the 670 km mantle discontinuity may provide direct evidence for horizontal shear along this boundary (cf. Kamiya et al., 1988; Shearer and Masters, 1992). Shear along the 670 km discontinuity also may be indicated by the general lack or break in continuity of seismicity from subducted lithosphere slabs beyond 700 km, implying solid phase transformations and possibly detachment and entrainment in convective lower mantle flow (McKenzie, 1983; Davies and Richards, 1992). Such an aseismic, detached lithospheric slab may have been tomographically imaged as a high velocity zone extending from 700 to 1700 km depth below North America (Grand, 1987). Hence, it is conceivable that shear along the 670 km boundary could produce longitudinal convective rolls instead of transverse convective rolls. Such an upper mantle convection mechanism would imply that convective rolls below the African Plate take a minimum of 20 Ma to become well developed. If such rolls were responsible for hotline development

in the Miocene, shear at the 670 km discontinuity would have had to been initiated in the Eocene.

Once longitudinal rolls become developed, convection also would have been produced parallel to the axes of these rolls. Below critical Rayleigh number (R_c), the velocity of flow at the fixed boundary layer, in this case the lithosphere–asthenosphere boundary, would be zero (Richter and Parsons, 1975). Above R_c, convective rolls would begin to produce shear at the L/A boundary layer, and if not accommodated by movement of this layer, would lead to bimodal and possibly multimodal patterns of convection. Such patterns of convection would then give rise to circular and ovoid-shaped swells in plan view.

This model implies that longitudinal convective rolls under West African volcanic chains could continue northeast, below African continental lithosphere. Neogene volcanic zones on the African continent are colored black in Fig. 9. We have projected inferred West African hotlines across the plate and there is some correlation to volcanism, although gaps have been noted where these lines cross Archean cratons that may have deep lithospheric roots (Fig. 9). This also is seen as NE–SW trends of low elastic thickness in continental Africa away from Archean cratons (Hartley et al., 1996). Uplift of the African continent by convective rolls also may help to explain elevated freeboard of the African continent since the Miocene (cf. Burke and Wilson, 1972; Bond, 1978; Morgan, 1983; Harrison, 1990).

An aspect ratio of horizontal to vertical diameter of cylindrical convective rolls would be greater than 1.0, using a hotline half-width spacing of 850 km and the 670 km discontinuity as a lower boundary layer. If oceanic lithosphere away from the Mid-Atlantic Ridge and post Archean continental lithosphere of the African plate are assumed to be ~100 km, this leaves ~570 km for the vertical diameter of convective rolls above the 670 km discontinuity. Assuming no horizontal gaps between adjacent upgoing and downgoing currents between rolls, the aspect ratio would be ~1.5. Aspect ratios of 1.0 could be achieved if a zone of turbulent mixing 140 km wide separated uprising and downgoing currents. This gap, however, is too broad to expect a convective system to be maintained by unidirectional shear at a boundary layer. Aspect ratios of 1.0 could alternatively be achieved by extending the lower boundary layer to 950 km. This depth is hard to reconcile, because the change in physical properties across the 670 km discontinuity would preclude free circulation across this boundary. It is more reasonable to accept that inferred convective rolls have return flow at the 670 km discontinuity and aspect ratios of ~1.5. This idea is demonstrated in Fig. 10.

A scenario for formation of hotlines and swells below the African plate as a result of longitudinal rolls is presented as follows: Initial upper mantle convection began in the Eocene from NE-oriented shear, and possibly from increased heating below the 670 km discontinuity due to changing convective currents in the lower mantle. This upper mantle convection took the form of NE-oriented cylindrical cells, with aspect ratios close to 1.5. By the Late Oligocene, convective rolls initiated hotline manifestations in the lithosphere by dynamic uplift and accumulation of melts released by mantle decompression. Refertilized mantle, enriched in LILE and radiogenic Sr and Pb from subducted material, residing at the 670 km discontinuity (Ringwood, 1982; Davies et al., 1989) began to ascend and release partial melt, which then metasomatized shallower mantle during ascent. Zones of mantle underplating and dynamic uplift were unevenly spaced along the length of these hotlines. Tension from divergent upwelling between rolls (Richter, 1973) began to open zones of preexisting weakness in the lithosphere, and these structures acted as conduits for early melts. Continued convective heating by addition of hot mantle to the lithosphere above upwelling zones began to cause the lithosphere to weaken and yield to upward stress. Sinistral, transcurrent shear (Lameyre et al., 1984) may have been produced along the CVL as a response to Alpine intraplate stress or differential flow rates in the longitudinal direction between convective rolls. Rayleigh–Taylor instabilities forming along the lengths of rising hotlines would have developed into discrete diapirs or a bimodal pattern of diapiric upwelling that gave rise to the main volcanic centers (see the filtered gravity map of Marsh and Marsh, 1976, their fig. 5) shows NNE- and NW-oriented lineations in gravity anomalies across the African plate, which could represent bimodal to multimodal upper mantle convection). By the Middle Miocene, the lithosphere along the hot-

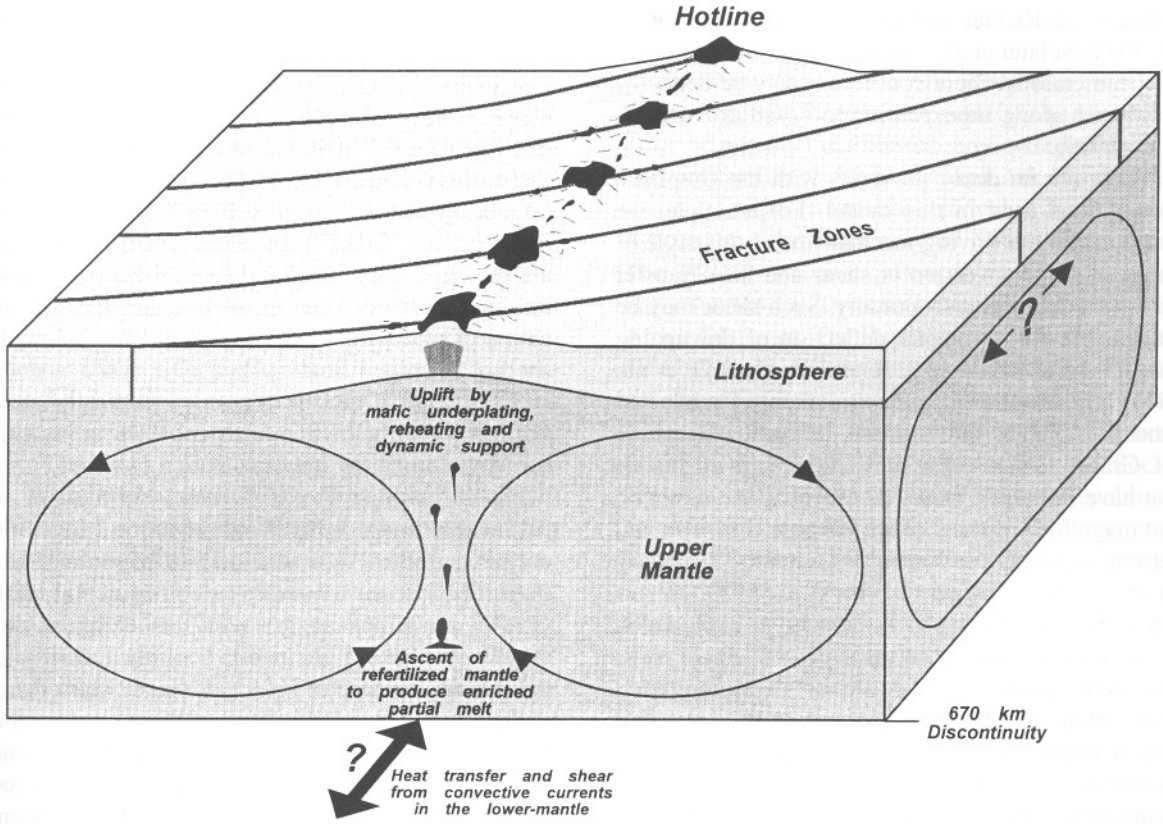

Fig. 10. Model illustrating hotline formation by Rayleigh–Benard convection in the upper mantle. Cylindrical, longitudinal convective rolls are generated in the upper mantle by heat transfer across and shear along the 670 km discontinuity from convective currents in the lower mantle. Horizontal to vertical aspect ratios of these convective rolls are 1.5. Hotlines form above upgoing currents between these rolls, where refertilized mantle from the 670 km discontinuity gives rise to enriched partial melt. Dynamic uplift from the rising mantle, intrusion by mafic partial melt, and reheating all contribute to uplift of the lithosphere along the hotline.

line was uplifted to form a series of swells where volcanism was most vigorous. Hotline lithosphere in between these swells was also affected by a smaller degree of uplift and volcanism. This could explain the proximity between the Cape Verde Rise and Canary rise within overlapping plume (?) diameters, seamounts between them on the topography/gravity maps calculated from Seasat, Geosat and ERS-1 data (Haxby, 1987; Smith and Sandwell, 1997), and a low S-wave velocity channel between them (Tanimoto and Zhang, 1992).

Our model of upper mantle convective rolls also provides an explanation for less depleted OIB for the CVL and possibly other inferred West African hotlines. This model explains more radiogenic, upper mantle $^{87}Sr/^{86}Sr$ and $^{206}Pb/^{204}Pb$ ratios found in CVL igneous rocks by providing a convection mechanism to transfer partial melt extracted from refertilized mantle residing at the 670 km discontinuity (cf. Ringwood, 1982; Ringwood et al., 1992). Pressure decrease during ascent would have caused increased partial melting and further enrichment. Melt fractionation and release of volatiles during ascent also would have caused metasomatism of shallower mantle, as has been documented for mantle xenoliths from the CVL (Fitton and Dunlop, 1985; Halliday et al., 1988; Lee et al., 1996).

Our model also provides a mechanism for maintenance of heatflow to the base of the plate. Localized stirring of the upper mantle would distribute heat to the base of the plate, producing stable heatflow in old oceanic lithosphere, elevated heatflow along

hotlines (cf. Richter and Parsons, 1975; Herman et al., 1977; Sclater et al., 1981), and lower heatflow in Archean cratons where convection may be deflected downward along lithospheric roots (see also Davies et al., 1989).

There are no doubt problems with the simplistic assumptions used in this model. For example, we propose that the driving mechanism for this style of upper mantle convection is shear and heat transfer across the 670 km discontinuity. Such shear may be responsible for horizontal deflection of downgoing lithosphere at subduction zones (cf. Kamiya et al., 1988) and detachment and entrainment of subducted lithospheric slabs into currents in the lower mantle (cf. Grand, 1987). Yet, at present there are no studies that have been able to directly identify the direction and magnitude of shear proposed here (Fig. 10), and current ideas on the viscosity of mantle boundary layers are wide ranging (Davies et al., 1989; Davies and Richards, 1992). Also, there is no explanation as to what occurs at the ends of convective rolls, and there should be evidence of swell migration if the plate drifted over upper mantle convective cells (Crough, 1983). For now, we will assume that convective rolls terminated as instabilities at plate boundaries, because our model involves a sensitive balance of upper mantle convection that is secondary to mechanisms driving relative plate motions. We also ignore mineral phase changes (olivine to spinel) and viscosity changes at the 410 km discontinuity; although this phase boundary may only be caused by minor physio chemical changes (Ita and Stixrude, 1992) and does not appear to have a profound effect on descending slabs of subducted lithosphere (McKenzie, 1983; Allen and Allen, 1990; Shearer and Masters, 1992).

8. Conclusions

Interpretation of WAPS MCS and gravity data show that CVL islands and seamounts are comprised of uplifted oceanic basement, thick pre-Miocene sedimentary overburden, and Neogene volcanic cover. Reheating and volcanism may have begun in the Oligocene, but uplifting of the lithosphere and volcanism were most active during the Miocene. In the brittle upper crust, uplift was primarily accommodated by ductile creep following reheating and small-offsets along numerous sub-vertical faults; though some uplift is documented along steep, normal faults that may be reactivated oceanic fracture zones. Coeval Miocene crustal uplift extends from São Tomé (and Pagalu, cf. Grunau et al., 1975) into the onshore portion of the CVL, and rules out the possibility that this portion of the CVL represents a hotspot trace. Other features evident from our data are the apparently preferential occurrence of crustal uplifts at fracture zone crossings, and the identification of pluton-like features in the crust below the shelf of Príncipe Island.

Interpreted WAPS MCS profiles show uplifted reflection Moho below the flanks of CVL seamounts; the Moho boundary may maintain a constant crustal thickness through the CVL axis, but it was not seismically imaged. Uplift of reflection Moho with oceanic basement indicates to us an anomalous mantle form of isostatic compensation for crustal uplift. Gravity modelling suggests that an elongate, NE-trending wedge of light mantle possibly underlies the uplifted lithosphere at Príncipe Island. Mass deficit within this light, anomalous mantle is suggested to be produced by a combination of intruded mafic material, thermal expansion from reheating, and possibly dynamic uplift from upwelling asthenosphere. Our proposed mechanism for uplift, volcanism and reheating involves discontinuous intrusion of partial melt at the base of the lithosphere below the entire length of the CVL, possibly as far southwest as St. Helena Island, and dynamic uplift over a mantle 'hotline'.

Although many workers consider the CVL and other West African volcanic island chains and swells with similar trends (Canary Islands, Cape Verde Rise, Sierra Leone Rise, Walvis Ridge) to be hotspot traces, the geological characteristics shared between these linear volcanic belts are quite different from the Hawaiian paradigm. The volcanic centers and inter-island ridges are not entirely made up of thick piles of intraplate volcanics, but are instead combinations of uplifted lithosphere and considerably less volcanic material, and hence are not surrounded by flexural moats. Furthermore, the West African linear volcanic chains have similar: crustal structure, elevated heatflow along their lengths, evidence for increased crustal uplift and volcanism in the Miocene, and parallel trends with ~1700 km separation. These

similarities have lead us to consider that these features may be related by convection currents in the upper mantle.

We propose that West African linear volcanic chains form parallel hotlines that are products of mantle upwelling between Rayleigh–Bernard-type cylindrical convective rolls formed in the upper mantle. The driving force for these convective rolls could have been a combination of heat transfer across and unidirectional shear along the 670 km discontinuity from convective currents in the lower mantle. Such a convection mechanism can be used to explain enriched LILE, radiogenic Sr and Pb, and similar trace element chemistries along hotlines by upwelling and partial melting of refertilized mantle originating at the 670 km discontinuity. Creation of localized swells by Rayleigh–Taylor instability and focusing of asthenosphere upwelling at fracture zone crossings may explain uneven distribution of volcanism and uplift along some of these inferred hotlines.

Our hypothesis that West African volcanic chains and possibly volcanics on the African continent are produced by upper mantle, Rayleigh–Bernard convection should be regarded as speculative, but cannot entirely be discounted using existing data. It is intended to provide an alternative to the hotspot theory, where age progression and subsidence along linear volcanic chains does not occur. Existence of long-lived mantle hotspots may still hold true for West African volcanic chains, other than the CVL, but the idea that volcanic centers along the CVL represent fixed reference points for studying plate motions over hotspots should be reexamined. This is not an attempt to provide an alternative hypothesis to deep mantle plumes for features such as the Hawaiian–Emperor chain and East Greenland–Iceland plume, both of which show well-documented age progressions, thick volcanic constructions, and subsidence following thermal rejuvenation over a circular source.

While there are not many well-documented flood basalt provinces of Miocene age, the global abundance of uplifted swells and volcanic centers during this time may have been overlooked as being a product of a global mantle event having a subtle effect on global sea level and paleotemperature (cf. Larson, 1991).

Acknowledgements

The West African PROBE Study is a joint venture with JEBCO Seismics and GECO-PRAKLA. Data acquisition and initial processing were carried out by GECO-PRAKLA and Ark Geophysical. Financial support has been provided by Agip and Amoco, and the University of Miami Bader Fund. The PROBE seismic processing system was partially funded by Texaco (Latin America and West Africa Division). The Republics of Cameroon, Equatorial Guinea, Gabon and São Tomé and Príncipe gave permission for access to their territorial waters and ports. We wish to thank Project PROBE workers at the University of Miami, AGSO and Sociéte Nationale des Hydrocarboures in the Republic of Cameroon who participated in the WAPS program: Deborah Scott, Henny Groschel-Becker, Kurt Kaczmarick, Richard Seme-Abomo and Americo Neves-Rosa. The authors also wish to thank the following individuals for reviewing this manuscript: Trevor Beardsmore, James Austin, Jr., Peter Rona, Gregor Eberli, J. Derek Fairhead, Adolph Nicolas, Godfrey Fitton and F. Wenzel.

References

Allen, P.A., Allen, J.R., 1990. Basin Analysis, Principles and Applications. Blackwell, Oxford, 451 pp.

Ambeh, W.B., Fairhead, J.D., 1991. Regular, deep seismicity beneath Mt. Cameroon volcano: lack of evidence for tidal triggering. Geophys. J. Int. 106, 287–291.

Ambeh, W.B., Fairhead, J.D., Francis, D.J., Nnange, J.M., Djallo, S., 1989. Seismicity of the Mount Cameroon region, West Africa. J. Afr. Earth Sci. 9, 1–7.

Armstrong, A.C., 1985. Oil and gas developments in central and southern Africa in 1984. AAPG Bull. 69, 1680–1726.

Baker, I., Gale, N.H., Simons, J., 1967. Geochronology of the St. Helena volcanoes. Nature 215, 1451–1456.

Baker, P.E., 1973. Islands of the south Atlantic. In: Nairn, A.E.M., Stehli, F.G. (Eds.), The Ocean Basins and Margins, Vol. 1. Plenum Press, New York, NY, pp. 493–553.

Basile, C., Mascle, J., 1990. Block faulting in oceanic crust: Examples of intraplate deformation in the Equatorial Atlantic. Mar. Geol. 95, 45–50.

Baudry, N., Kroenke, L., 1991. Intermediate-wavelength (400–600 km), South Pacific geoidal undulations: their relationship to linear volcanic chains. Earth Planet. Sci. Lett. 102, 430–443.

Benkhelil, J., 1989. The origin and evolution of the Cretaceous Benue Trough (Nigeria). J. Afr. Earth Sci. 8, 251–282.

Binks, R.M., Fairhead, J.D., 1992. A plate tectonic setting for

Mesozoic rifts of West and Central Africa. Tectonophysics 213, 141–151.

Bonatti, E., Harrison, C.G.A., 1976. Hot lines in the earth's mantle. Nature 263, 402–404.

Bonatti, E., Harrison, C.G.A., Fisher, D.E., Honnorez, J., Schilling, J.-G., Stipp, J.J., Zentilli, M., 1977. Easter volcanic chain (southeast Pacific): A mantle hotline. J. Geophys. Res. 82, 2457–2478.

Bond, G., 1978. Evidence for late Tertiary uplift of Africa relative to North America, South America, Australia and Europe. J. Geol. 86, 47–65.

Bott, M.H.P., 1981. Crustal doming and the mechanism of continental rifting. Tectonophysics 73, 1–8.

Bott, M.H.P., Kusznir, N.J., 1979. Stress distribution associated with compensated plateau uplift structures with application to the continental splitting mechanism. Geophys. J. R. Astron. Soc. 56, 451–459.

Burke, K., 1969. Seismic areas of the Guinea coast where Atlantic fracture zones reach Africa. Nature 222, 655–657.

Burke, K., Wilson, J.T., 1972. Is the African plate stationary? Nature 239, 387–389.

Cantagrel, P.J.M., Jamond, C., Lasserre, M., 1978. Le magnetisme alcalin de la ligne du Cameroun au Tertiare inferieur: donnees geochronologiques K/Ar. Soc. Geol. Fr. 6, 300–303.

Cornen, G., Maury, R.C., 1980. Petrology of the volcanic island of Annobon, Gulf of Guinea. Mar. Geol. 36, 253–267.

Courtney, R.C., White, R.S., 1986. Anomalous heat flow and geoid across the Cape Verde Rise: evidence for dynamic support from a thermal plume in the mantle. Geophys. J. R. Astron. Soc. 87, 815–867.

Crough, S.T., 1978. Thermal origin of mid-plate hot-spot swells. Geophys. J. R. Astron. Soc. 5, 451–469.

Crough, S.T., 1983. Hotspot swells. Annu. Rev. Earth Planet. Sci. 11, 165–193.

Davies, G.F., Richards, M.A., 1992. Mantle convection. J. Geol. 100, 151–206.

Davies, G.R., Norry, M.J., Gerlach, D.C., Cliff, R.A., 1989. A combined chemical and Pb–Sr–Nd isotope study of the Azores and Cape Verde hot spots: the geodynamical implications. In: Saunders, A.D., Norry, M.J. (Eds.), Magmatism in the Ocean Basins. Geol. Soc. London Spec. Publ. 42, 231–255.

Delmas, M., 1982. São Tomé (Golf de Guinee), Perspectives petrolieres. Soc. Nat. Elf Aquitaine, Rep. 192/82, 31.

Déruelle, B., N'ni, J., Kambou, R., 1987. Mount Cameroon: An active volcano of the Cameroon line. J. Afr. Earth Sci. 6, 197–214.

Detrick, R.S., Crough, S.T., 1978. Island subsidence, hot spots, and lithospheric thinning. J. Geophys. Res. 83, 1236–1244.

Detrick, R.S., Watts, A.B., 1979. An analysis of isostasy in the world's oceans 3. Aseismic ridges. J. Geophys. Res. 84, 3637–3653.

Downes, H., 1990. Shear zones in the upper mantle — Relation between geochemical enrichment and deformation in mantle peridotites. Geology 18, 374–377.

Duncan, R.A., Richards, M.A., 1991. Hotspots, mantle plumes, flood basalts, and true polar wander. Rev. Geophys. 29, 31–50.

Dunlop, H.M., Fitton, J.G., 1979. A K–Ar and Sr-isotopic study of the volcanic rocks of the island of Príncipe, West Africa — Evidence for mantle heterogeneity beneath the Gulf of Guinea. Contrib. Mineral. Petrol. 71, 125–131.

Dumort, J.C., 1968. Notice explicative sur la feuille Douala-ouest. Géol. Bur. Rech. Géol. Minières, Republic of Cameroon, 69 pp.

Emery, K.O., Uchupi, E., Phillips, J., Brown, C., Mascle, J., 1975. Continental margin off West Africa: Angola to Sierra Leone. AAPG Bull. 59, 2209–2265.

Ewing, M., Le Pichon, X., Ewing, J., 1966. Crustal structure of the mid-ocean ridges, 4. Sediment distribution in the South Atlantic Ocean and the Cenozoic history of the Mid-Atlantic ridge. J. Geophys. Res. 71, 1611–1636.

Fairhead, J.D., 1988. Mesozoic plate reconstructions of the central south Atlantic Ocean: The role of west and central African rift system. Tectonophysics 155, 181–191.

Fairhead, J.D., Binks, R.M., 1991. Differential opening of the Central and South Atlantic Oceans and the opening of the West African rift system. Tectonophysics 187, 191–203.

Fairhead, J.D., Okereke, C.S., 1988. Depths to major density contrasts beneath the West African rift system in Nigeria and Cameroon based on the spectral analysis of gravity data. J. Afr. Earth Sci. 7, 769–777.

Fitton, J.G., 1980. The Benue trough and Cameroon line — A migrating rift system in West Africa. Earth Planet. Sci. Lett. 51, 132–138.

Fitton, J.G., 1983. Active versus passive continental rifting: Evidence from the West African rift system. Tectonophysics 94, 473–481.

Fitton, J.G., Dunlop, H.M., 1985. The Cameroon line, West Africa, and its bearing on the origin of oceanic and continental alkali basalt. Earth Planet. Sci. Lett. 72, 23–38.

Fowler, C.M.R., 1992. The Solid Earth, an Introduction to Global Geophysics. Cambridge Univ. Press, New York, NY, 472 pp.

Francheteau, J., Le Pichon, X., 1972. Marginal fracture zones as structural framework of continental margins in the South Atlantic Ocean. AAPG Bull. 56, 991–1007.

Gamboa, L.A.P., Ganey, P., Buffler, R.T., 1983. Erosion and progradation in the deep sea — Examples from the western South Atlantic. In: Bally, A.W. (Ed.), Seismic Expressions of Structural Styles — a Picture and Work Atlas. Am. Assoc. Pet. Geol., Stud. Geol. 15 (2), 1.2.2-19–1.2.2-25.

Goldflam, P., Hinz, K., Weigel, W., Wissmann, G., 1980. Some features of the northwest African margin and magnetic quiet zone. R. Soc. London Philos. Trans., Ser. A 294, 87–96.

Goslin, J., Sibuet, J.C., 1975. Geophysical study of the easternmost Walvis Ridge, South Atlantic: Deep structure. Geol. Soc. Am. Bull. 86, 1713–1724.

Goslin, J., Mascle, J., Sibuet, J.C., Hoskins, H., 1974. Geophysical study of the easternmost Walvis Ridge, South Atlantic: Morphology and shallow structure. Geol. Soc. Am. Bull. 85, 619–632.

Gorini, M.A., Bryan, G.M., 1976. The tectonic fabric of the equatorial Atlantic and adjoining continental margins: Gulf of Guinea to northeastern Brazil. An. Acad. Brasil. Cienc. 48, 101–119.

Grand, S.P., 1987. Tomographic inversion for shear velocity be-

neath the North American Plate. J. Geophys. Res. 29, 14065–14090.

Gripp, A.E., Gordon, R.G., 1990. Current plate velocities relative to the hotspots incorporating the NUVEL-1 global plate motion model. Geophys. Res. Lett. 17, 1109–1112.

Grunau, H.R., Lehner, P., Cleintuar, M.R., Allenbach, P., Bakker, G., 1975. New radiometric ages and seismic data from Fuerteventura (Canary Islands), Maio (Cape Verde Islands), and São Tomé (Gulf of Guinea). In: Borradaile, G.J., Ritsema, A.R., Rondeel, H.E., Simon, O.J. (Eds.), Progress in Geodynamics. North-Holland, New York, NY, pp. 90–118.

Halliday, A.N., Dickin, A.P., Fallick, A.E., Fitton, G., 1988. Mantle dynamics: a Nd, Sr, Pb and O isotope study of the Cameroon line volcanic chain. J. Petrol. 29, 181–211.

Halliday, A.N., Davidson, J.P., Holden, P., DeWolf, C., Lee, D.C., Fitton, G., 1990. Trace-element fractionation in plumes and the origin of HIMU mantle beneath the Cameroon line. Nature 347, 523–528.

Harrison, C.G.A., 1990. Long-term eustacy and epeirogeny in continents. In: Revelle, R.R. (Ed.), Sea-Level Change. National Academy Press, Washington, DC, pp. 141–158.

Hartley, R., Watts, A.B., Fairhead, J.D., 1996. Isostasy of Africa. Earth Planet. Sci. Lett. 137, 1–18.

Haxby, W.F., 1987. Gravity Field of the World's Oceans. Natl. Geophys. Data Center, Boulder, CO, 1 sheet.

Hedberg, J.D., 1969. A geological analysis of the Cameroon trend. Ph.D. Thesis, Princeton Univ., 188 pp.

Herman, B.M., Langseth, M.G., Hobart, M.A., 1977. Heat flow in the oceanic crust bounding western Africa. Tectonophysics 41, 61–77.

Hinz, K., 1981. A hypothesis on terrestrial catastrophes, wedges of very thick oceanward dipping layers beneath passive continual margins — their origin and paleoenvironmental significance. Geol. Jahrb. Reihe E 23, 3–28.

Holik, J.S., Rabinowitz, P.D., Austin, J.A.Jr., 1991. Effects of Canary hotspot volcanism on structure of oceanic crust off Morocco. J. Geophys. Res. 96, 12039–12067.

Ita, J., Stixrude, L., 1992. Petrology, elasticity, and composition of the mantle transition zone. J. Geophys. Res. 97, 6849–6866.

Jacobs, G.K., Dunbar, N.W., Naney, M.T., Williams, R.T., 1992. Petrologic and geophysical studies of an artificial magma chamber. Eos 73, 401, 411–412.

Jansa, L.F., Pe-Piper, G., 1988. Middle Jurassic to Early Cretaceous igneous rocks along eastern North American continental margin. AAPG Bull. 72, 347–366.

Kamiya, S., Miyatake, T., Hirahara, K., 1988. How deep can we see the high velocity anomalies beneath the Japan Islands? Geophys. Res. Lett. 15, 828–831.

Keen, C.E., 1988. The dynamics of rifting: deformation of the lithosphere by active and passive driving forces. Geophys. J. R. Astron. Soc. 80, 95–120.

Kellogg, J.N., Wedgeworth, B.S., Freymueller, J., 1987. Isostatic compensation and conduit structures of western Pacific seamounts: results of three-dimensional gravity modelling. In: Keating, B.H., Fryer, P., Batiza, R., Boehlert, G.W. (Eds.), Seamounts, Islands and Atolls. Am. Geophys. Union, Geophys. Monogr. 43, 85–96.

Lameyre, J., Black, R., Bonin, B., Giret, A., 1984. Les provinces magmatiques de l'Est américain, de l'Ouest africain et des Kerguelen. Indications d'un contrôle tectonique et d'une initiation superficielle du magmatisme intraplate et des processus associés. Soc. Géol. Nord Ann. 103, 101–114.

Lancelot, Y., Seibold, E., 1978. The evolution of the central northeastern Atlantic — Summary of results of DSDP Leg 41. Init. Rep. DSDP 41, 1215–1245.

Larson, R.L., 1991. Geological consequences of superplumes. Geology 19, 963–966.

Lee, D.-C., Halliday, A.N., Fitton, J.G., Poli, G., 1994. Isotopic variations with distance and time in the volcanic islands of the Cameroon line. Earth Planet. Sci. Lett. 123, 119–139.

Lee, D.-C., Halliday, A.N., Davies, G.R., Essente, E.J., Fitton, J.G., Temdjim, R., 1996. Melt enrichment of shallow depleted mantle: a detailed petrological, trace element and isotopic study of mantle-derived xenoliths and megacrysts from the Cameroon line. J. Petrol. 37, 415–441.

Lehner, P., de Ruiter, P.A.C., 1977. Structural history of Atlantic margin of Africa. AAPG Bull. 61, 961–981.

Lin, J., Purdey, G.M., Schouten, H., Sempere, J.-C., Zervas, C., 1990. Evidence from gravity data for focused magmatic accretion along the Mid-Atlantic Ridge. Nature 344, 627–632.

Lo, P.G., Dia, A., Kampunzu, A.B., 1992. Cenozoic volcanism and its relationship to the opening of the central Atlantic Ocean. Tectonophysics 209, 281–291.

Marsh, B.D., Marsh, J.G., 1976. On global gravity anomalies and two-scale mantle convection. J. Geophys. Res. 81, 5267–5280.

McKenzie, D.P., 1983. The earth's mantle. Sci. Am. 249, 66–113.

McNutt, M., 1988. Thermal and mechanical properties of the Cape Verde Rise. J. Geophys. Res. 93, 2784–2794.

Meyers, J.B., Rosendahl, B.R., 1991. Seismic reflection character of the Cameroon Volcanic Line: Evidence for uplifted oceanic crust. Geology 19, 1072–1076.

Meyers, J.B., Rosendahl, B.R., Groschel-Becker, H., Austin, J.A.Jr., Rona, P., 1996. Deep penetrating MCS imaging of the rift-to-drift transition, offshore Douala and North Gabon basins, West Africa. Mar. Pet. Geol. 13, 791–835.

Moreau, C., Regnoult, J., Déruelle, B., Robineau, B., 1987. A new tectonic model for the Cameroon line, central Africa. Tectonophysics 142/139, 317–334.

Morgan, W.J., 1972. Plate motions and deep mantle convection. In: Shagam, R., Hargraves, R.B., Morgan, W.J., Van Houten, R.B., Burk, C.A., Holland, H.D., Hollister, L.C. (Eds.), Studies in Earth and Space Sciences. Geol. Soc. Am. Mem. 123, 7–22.

Morgan, W.J., 1983. Hotspot tracks and the early rifting of the Atlantic. Tectonophysics 94, 123–139.

Musgrove, L.A., Austin, J.A., 1984. Multichannel seismic reflection survey of the southeast Angola basin. Init. Rep. DSDP 75, 1191–1210.

Nicolas, A., 1989. Structures of Ophiolites and Dynamics of Oceanic Lithosphere. Kluwer, Dordrecht, 367 pp.

O'Connor, J.M., Duncan, R.A., 1990. Evolution of the Walvis Ridge–Rio Grande rise hot spot system: Implications for African and South American plate motions over plumes. J. Geophys. Res. 95, 17475–17502.

O'Connor, J.M., Le Roex, A.P., 1992. South Atlantic hot spot-plume systems: 1. Distribution of volcanism in time and space. Earth Planet. Sci. Lett. 113, 343–364.

Okereke, C.S., 1988. Contrasting modes of rifting: The Benue trough and Cameroon Volcanic Line, West Africa. Tectonics 7, 775–784.

Piper, J.D.A., Richardson, A., 1972. The paleomagnetism of the Gulf of Guinea volcanic province, West Africa. Geophys. J. R. Astron. Soc. 29, 147–171.

Poudjom-Djomani, Y.H., Diament, M., Albouy, Y., 1992. Mechanical behavior of the lithosphere beneath the Adamawa uplift (Cameroon, West Africa) based on gravity data. J. Afr. Earth Sci. 15, 81–90.

Poudjom-Djomani, Y.H., Nnange, J.M., Diamet, M., Ebinger, C.J., Fairhead, J.D., 1995. Effective elastic thickness and crustal thickness variations in west central Africa inferred from gravity data. J. Geophys. Res. 100, 22047–22070.

Rabinowitz, P.D., LaBrecque, J., 1979. The Mesozoic South Atlantic Ocean and evolution of its continental margins. J. Geophys. Res. 84, 5973–6002.

Regnoult, J.M., 1986. Synthèse géologique du Cameroon. Dir. Mines Géol., Republic of Cameroon, 119 pp.

Reyre, D., 1966. Histoire géologique du bassin de Douala (Cameroun). In: Reyre, D. (Ed.), Sedimentary Basins of the African Coasts, Part 1: Atlantic Coast. Assoc. Afr. Geol. Surv., Paris, pp. 143–160.

Richter, F.M., 1973. Convection and the large-scale circulation of the mantle. J. Geophys. Res. 78, 8735–8745.

Richter, F.M., Parsons, B., 1975. On the of two scales of convection in the mantle. J. Geophys. Res. 80, 2529–2541.

Ringwood, A.E., 1982. Phase transfromations and differentiation in subducted lithosphere: implications for mantle dynamics, basalt petrogenesis and crustal evolution. J. Geol. 90, 611–643.

Ringwood, A.E., Kesson, S.E., Hibberson, W., Ware, N., 1992. Origin of kimberlites and related magmas. Earth Planet. Sci. Lett. 113, 521–538.

Robertson, A.H.F., Bernoulli, D., 1982. Stratigraphy, facies, and significance of Late Mesozoic and early Tertiary sedimentary rocks of Fuerteventura (Canary Islands) and Maio (Cape Verde Islands). In: Von Rad, U., Hinz, K., Sarnthein, M., Seibold, E. (Eds.), Geology of the Northwest African Continental Margin. Springer, New York, NY, pp. 498–525.

Rohrman, M., Van der Beek, P., 1996. Cenozoic postrift domal uplift of North Atlantic margins: and Asthenospheric diapirsm model. Geology 24, 901–904.

Rothe, P., 1990. Sediments of volcanic islands — On the importance of the exception. In: Heling, D., Rothe, P., Stoffers, P. (Eds.), Sediments and Environmental Chemistry, Selected Aspects and Case Histories. Springer, New York, NY, pp. 29–47.

Schmincke, H.U., 1982. Volcanic and chemical evolution of the Canary Islands. In: Von Rad, U., Hinz, K., Sarnthein, M., Seibold, E. (Eds.), Geology of the Northwest African Continental Margin. Springer, New York, NY, pp. 273–306.

Schouten, H., Whitehead, J., 1991–1992. Modelling ridge segmentation .... Oceanus 34, 19–20.

Sclater, J.G., Parsons, B., Jaupart, C., 1981. Oceans and continents: Similarities and differences in the mechanisms of heat loss. J. Geophys. Res. 86, 11535–11552.

Scotese, C.R., Gahagan, L.M., Larson, R.L., 1988. Plate tectonic reconstructions of the Cretaceous and Cenozoic basins. Tectonophysics 155, 27–48.

Shearer, P.M., Masters, T.G., 1992. Global mapping of topography on the 660-km discontinuity. Nature 355, 791–796.

Sheridan, R.E., Houtz, R.E., Drake, C.L., Ewing, M., 1969. Structure of continental margin off Sierra Leone, West Africa. J. Geophys. Res. 74, 2512–2531.

Sibuet, J.-C., Mascle, J., 1978. Plate kinematic implications of Atlantic equatorial fracture zone trends. J. Geophys. Res. 83, 3401–3421.

Sibuet, J.-C., Hay, W.W., Prunier, A., Montadert, L., Hinz, K., Fritsch, J., 1984. The eastern Walvis Ridge and adjacent basins (South Atlantic): morphology, stratigraphy, and structural evolution in light of the results of legs 40 and 75. Init. Rep. DSDP, 483–508.

Smith, W.H.F., Sandwell, D.T., 1997. Measured and estimated seafloor topography. World Data Center-A for Marine Geology and Geophysics Research Publication RP-1, poster.

Stillman, C.J., 1987. A Canary Islands dike swarm: Implications for the formation of ocean islands by extensional fissural volcanism. In: Halls, H.C., Fahrig, W.F. (Eds.), Mafic Dike Swarms. Geol. Assoc. Can. Spec. Pap. 34, 243–255.

Stillman, C.J., Furnes, H., Le Bas, M.J., Robertson, A.H.F., Zielonka, J., 1982. The geological history of Maio, Cape Verde Islands. J. Geol. Soc. London 139, 347–361.

Stuart, G.W., Fairhead, J.D., Dorbath, L., Dorbath, C., 1985. A seismic refraction study of the crustal structure associated with the Adamawa plateau and Garoua rift, Cameroon, West Africa. Geophys. J. R. Astron. Soc. 81, 1–12.

Talwani, M., Worzel, J.L., Landisman, M., 1959. Rapid gravity computations for two-dimensional bodies with application to the Mendocino submarine fracture zone. J. Geophys. Res. 64, 49–59.

Tanimoto, T., Zhang, Y.S., 1992. Cause of low velocity anomaly along the South Atlantic hotspots. Geophys. Res. Lett. 19, 1567–1570.

Tissot, B., Demaison, G., Masson, P., Delteil, J.R., Conbaz, A., 1980. Paleoenvironment and petroleum potential of middle Cretaceous black shales in Atlantic basins. AAPG Bull. 64, 2051–2063.

Van der Linden, W.J.M., 1980. Walvis Ridge, a piece of Africa? Geology 8, 417–421.

Vogt, P.R., 1974. Volcano spacing, fractures, and thickness of the lithosphere. Earth Planet. Sci. Lett. 21, 235–252.

Vogt, P.R., 1991. Bermuda and Appalachian–Labrador rises: Common non-hotspot processes? Geology 19, 41–44.

Watkins, J.S., Hoppe, K.W., 1978. Seismic reflection reconnaissance of the Atlantic Margin of Morocco. In: Talwani, M., Hay, W.W., Ryan, W.B.F. (Eds.), Deep Drilling Results in the Atlantic Ocean: Continental Margins and Paleoenvironment. Am. Geophys. Union, Washington, DC, pp. 205–217.

Watts, A.B., ten Brink, U.S., Buhl, P., Brocher, T.M., 1985. A

multichannel seismic study of lithospheric flexure across the Hawaiian–Emperor seamount chain. Nature 315, 105–111.

White, R., McKenzie, D., 1989. Magmatism at rift zones: The generation of continental margins and flood basalts. J. Geophys. Res. 94, 7685–7729.

White, W.M., 1985. Sources of oceanic basalts: Radiogenic isotopic evidence. Geology 13, 115–118.

Wilson, M., 1992. Magmatism and continental rifting during the opening of the South Atlantic Ocean: a consequence of Lower Cretaceous super-plume activity. In: Storey, B.C., Alabaster, T., Pankhurst, R.J. (Eds.), Magmatism and the Causes of Continental Break-up. Geol. Soc. Spec. Publ. 68, 241–255.

Withjack, M., 1979. A convective heat transfer model for lithospheric thinning and crustal uplift. J. Geophys. Res. 84, 3008–3022.

Wright, J.A., Louden, K.E., 1989. CRC Handbook of Seafloor Heat Flow. CRC Press, Boca Raton, FL, 498 pp.

Zhang, Y.S., Tanimoto, T., 1992. Ridges, hotspots and their interaction as observed in seismic velocity maps. Nature 355, 45–49.